Pore-water Extraction and Characterization: Benchmarking of the Squeezing and Adapted Isotope Diffusive Exchange Methods

NWMO-TR-2018-14 **October 2018**

Daniel Rufer & Martin Mazurek
Rock-Water Interaction, Institute of Geological Sciences, University of Bern

nwmo
NUCLEAR WASTE MANAGEMENT ORGANIZATION
SOCIÉTÉ DE GESTION DES DÉCHETS NUCLÉAIRES

Nuclear Waste Management Organization
22 St. Clair Avenue East, 6th Floor
Toronto, Ontario
M4T 2S3
Canada

Tel: 416-934-9814
Web: www.nwmo.ca

Pore-water Extraction and Characterization: Benchmarking of the Squeezing and Adapted Isotope Diffusive Exchange Methods

NWMO-TR-2018-14

October 2018

Daniel Rufer & Martin Mazurek
Rock-Water Interaction, Institute of Geological Sciences, University of Bern

Document History

Title:	Pore-water Extraction and Characterization: Benchmarking of the Squeezing and Adapted Isotope Diffusive Exchange Methods		
Report Number:	NWMO-TR-2018-14		
Revision:	R000	Date:	October 2018
Rock-Water Interaction, Institute of Geological Sciences, University of Bern			
Authored by:	Daniel Rufer and Martin Mazurek		
Verified by:	Martin Mazurek		
Nuclear Waste Management Organization			
Reviewed by:	Laura Kennell-Morrison		
Reviewed by:	Monique Hobbs		
Accepted by:	Paul Gierszewski		

Revision Summary		
Revision Number	**Date**	**Description of Changes/Improvements**
R000	2018-10	Initial issue

ABSTRACT

Title: **Pore-water Extraction and Characterization: Benchmarking of the Squeezing and Adapted Isotope Diffusive Exchange Methods**
Report No.: **NWMO-TR-2018-14**
Author(s): Daniel Rufer & Martin Mazurek
Company: Rock-Water Interaction, Institute of Geological Sciences, University of Bern
Date: October 2018

Abstract

The objective of this research is to benchmark the squeezing and adapted isotope diffusive exchange (AIDE) methods for low-porosity, high-salinity systems. To this end, samples of Queenston, Georgian Bay and Blue Mountain formation shale collected during characterization activities at the Bruce Nuclear Site, as well as samples of Opalinus Clay collected from the Mont Terri Underground Rock Laboratory, were equilibrated with water from an external reservoir, such that the chemical and isotopic composition of the pore water was known and could be used as a benchmark. After equilibration, the samples were subjected to squeezing and AIDE tests, and the results were compared with the benchmark compositions. The equilibration process was a central aspect and accomplishment of the project, requiring a specialized design in order to minimize potential artefacts and to limit equilibration times.

TABLE OF CONTENTS

LIST OF TABLES

Page

LIST OF FIGURES

Page

1. INTRODUCTION: OBJECTIVES AND SCOPE

High-pressure squeezing has been successfully applied to obtain pore waters from clay-rich Mesozoic rocks from northern Switzerland, including Opalinus Clay and adjacent units (Pearson et al. 2003, Fernández et al. 2014, Mazurek et al. 2015). The first water is generally obtained at pressures of 100–200 MPa. With increasing pressure, analytical artefacts are identified and are due to ion filtration (leading to decreasing concentrations of anions and monovalent cations) and pressure-induced dissolution of carbonate minerals (leading to increasing concentrations of bivalent cations). Comparisons with independent methods, such as ground-water data of pore waters sampled in situ led to the conclusion that the first water, obtained at the lowest pressure, is the best approximation of the in-situ pore-water composition (Mazurek et al. 2015, 2017).

The squeezing method has been shown to be feasible for samples with water contents >3 – 3.5 wt.%. Given the higher degree of consolidation, and therefore lower water content, in the Ordovician shale units of southern Ontario in comparison with Opalinus Clay, higher pressures are needed in order to obtain waters by squeezing. In a feasibility study, Mazurek et al. (2013) were able to obtain water from one out of three samples at a pressure of 500 MPa. The question arises to what degree this water is affected by the artefacts identified at higher pressures for the samples from the Swiss program.

The isotope diffusive exchange technique is an established method to quantify the water isotopic composition of clay-rich sedimentary rocks (Rogge 1997, Rübel et al. 2000). The high salinity of the pore waters from southern Ontario is an issue when it comes to the applicability of the method. de Haller et al. (2016) developed an adapted analytical protocol for high-salinity waters (AIDE = Adapted Isotope Diffusive Exchange), but to date it has not been further tested.

The objective of this project is to benchmark the squeezing and AIDE methods for low-porosity, high-salinity systems, such as the Ordovician shales of southern Ontario. To this end, samples were equilibrated with water from an external reservoir, such that the chemical and isotopic composition of the pore water was known and could be used as a benchmark. After equilibration, the samples were subjected to squeezing and AIDE tests, and the results were compared with the benchmark compositions.

The equilibration process is a central aspect of the project and required a special design in order to minimize potential artefacts and to limit equilibration times.

- Opalinus Clay and, to a more limited degree, the Ordovician shales from southern Ontario are swelling materials. In order to limit swelling, stiff diffusion cells had to be constructed that volumetrically confine the samples. Xiang et al. (2016) studied the effects of confining pressure on diffusion coefficients and concluded that the absence of any confinement leads to a substantial increase of diffusion coefficients related to changes in the microfabric.

- Pore waters in the Ordovician samples are highly saline and therefore corrosive. In order to avoid corrosion over the extended time of equilibration, no steel was used for parts of the diffusion cells that are in contact with water; instead, they were made of plastic and titanium.

- Samples for squeezing are up to 10 cm long, with a diameter of 5 cm. In order to reduce the equilibration time, the samples were cut into slices with a thickness of about 1.5 cm each.

They were re-assembled after equilibration. This means that for each sample about 6 diffusion cells were required.

2. MATERIALS AND METHODS

2.1 DRILL CORE SAMPLES

Four samples were used for the tests: three from the Ordovician shales from the Bruce nuclear site (southern Ontario) and one from the Opalinus Clay of the Mont Terri Underground Laboratory (Switzerland). Drill core diameters are 7.5 cm for the DGR samples and 10 cm for the Mont Terri sample. The mineralogical compositions and the water contents of all samples are listed in Table 1.

Table 1: Mineralogical Composition and Water Content of Studied Samples

Site	Borehole	Depth [m]	Unit	Wet water content [wt.%]	Quartz [wt.%]	Albite [wt.%]	K-feldspar [wt.%]	Calcite [wt.%]	Dolomite/ Ankerite	Siderite [wt.%]	Anhydrite [wt.%]	Pyrite [wt.%]	C_{org} [wt.%]	Clay minerals [wt.%]
Mont Terri	BDR-B7	9.45	Opalinus Clay	8.59	12	1.3	1.4	16	1	b.d.	b.d.	1.2	0.8	66
DGR, Bruce	DGR-3	527.11	Queenston Formation	2.97	25	0.9	2.9	14	9	b.d.	Trace	0.8	0.1	47
DGR, Bruce	DGR-3	586.84	Georgian Bay Formation	4.06	28	1.5	1.8	3	2	b.d.	b.d.	0.2	0.3	63
DGR, Bruce	DGR-4	637.03	Blue Mountain Formation	3.16	23	1.7	b.d.	6	0.6	b.d.	b.d.	3.1	1.1	65

b.d. = below detection

The rock cores were concentrically inserted into PE tubes with 11.5 cm inner diameter and a wall thickness of 0.5 cm. The resulting ring space of 0.75 cm thickness between tube and sample was then filled with epoxy (Sikadur-52). Polymerization peak temperature during hardening of the epoxy remained below 60 °C (measured on the outside of the PE tube). In order to prevent excessive polymerization-heat build-up in the 2 cm wide ring space of the DGR samples (due to their smaller diameter), a smaller tube with 8.2 cm inner diameter was first positioned concentrically in the 11.5 cm tubes, and the space between was filled with epoxy. After hardening and cooling of this epoxy, the rock core was embedded in the inner tube, resulting in a ring space 0.35 cm thick. While not directly measured, a polymerization peak temperature below that of the Mont Terri sample is expected due to the thinner ring space. The short transient temperature increase is considered not to affect the measured chemical and isotopic composition of the pore water.

The embedded rock cores were then scanned on an X-ray CT scanner at the Institute of Forensic Medicine of the University of Bern (Switzerland). The objective was to identify fractures that might have formed since core embedding. Indeed, some such fractures were

found and were epoxy-filled, with some trapped air (Figure 1). The CT scans allowed to select unfractured and therefore epoxy-free areas before cutting slices of suitable thickness (see Section 3.1) for the equilibration experiments.

Cutting was performed dry on a miter saw. Any salient or uneven cutting-surface features were sanded down using a belt grinder. Afterwards, the cut slices were immediately vacuum-sealed into Al-coated plastic (Figure 2). This resulted in exposures of the cutting surfaces to air between 3 and 21 minutes (median: 9 minutes).

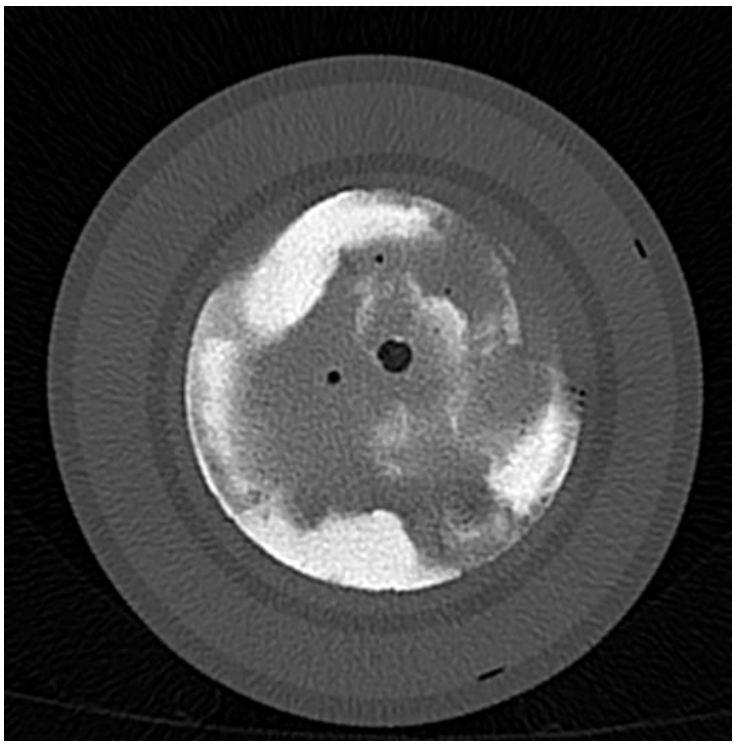

Notes: The image shows material density integrated over a 0.6 mm thick slice perpendicular to the core axis. Visible are the two concentric PE tubes (darker grey) used to embed the DGR samples. The sample inside the tubes shows a patchy pattern due to the undulating geometry of the bedding-parallel fracture plane. White areas indicate clay rock, grey areas show the resin-filled fracture within the studied slice. Black dots near the core axis are voids formed by air entrapped in the fracture plane during epoxy infiltration

Figure 1: CT Scan Slice of Sample DGR-3 586.84 Showing a Resin-filled Fracture

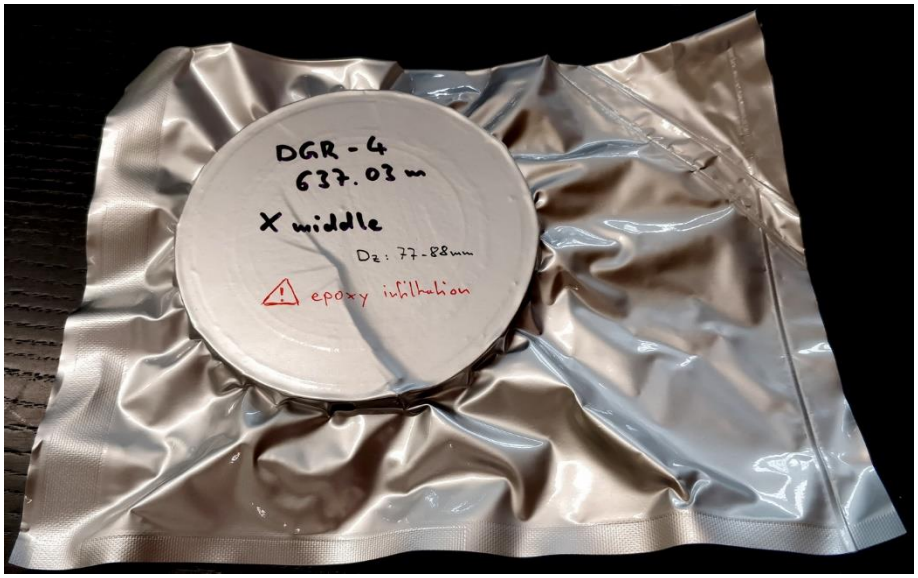

Figure 2: Illustration of a Rock Slice Vacuum-sealed in Al-coated Plastic

2.2 ARTIFICIAL PORE WATER (APW)

In order to minimize the equilibration times between pore water and the external reservoir, the chemical composition of the artificial pore water (APW) was chosen close to the best estimate of the pore-water composition. The Mont Terri sample is located along the same stratigraphic horizon as the PC-C pore water sampled in situ by Vinsot et al. (2008). The composition of the APW was formulated according to this water, but with a higher concentration of Br, which served as a conservative tracer to monitor the equilibration process between APW and pore water in the experiments. Table 2 summarizes the pertinent data.

The pore-water composition for the DGR samples is more difficult to constrain. The water squeezed from a sample of the Blue Mountain Formation was used as a proxy (Mazurek et al. 2013). It was suspected that the value for K in the squeezed water may be too low (substantial ion exclusion), so the value from the Guelph ground water was used (Heagle & Pinder 2009). The value for Ca is estimated on the basis of aqueous extraction data from the Blue Mountain Formation (Hobbs et al. 2011) because effects of calcite dissolution are expected for the squeezed sample (a pressure of 500 MPa was needed to obtain water). Cl based on squeezing was adjusted for charge balance.

Despite this, the fact remains that the DGR APW will not perfectly match the pore-water composition. This means that during equilibration two high-salinity waters will mix. Such mixing is likely to lead to precipitation, as inferred by Waber et al. (2007) for an advective-displacement experiment in which a decrease of hydraulic conductivity was observed over time. Furthermore, the preparation of a high-salinity APW is an issue in itself and may also lead to precipitation. For these reasons, the salinity of the APW was reduced to about 50 % of the estimated value, i.e. all ion concentrations were halved. Two APWs were prepared, one of them with a high Br content of 5000 mg/kg, again serving as a conservative tracer to monitor the equilibration progress. All pertinent data are summarized in Table 3.

Table 2: Composition of the Mont Terri APW

	Mont Terri PC-C water Vinsot et al. (2008, Tab. 3, average)			APW	
	Original data [mmol/kg*]	Recalculated to [mg/kg]	Original data, with added Br [mmol/kg]	APW recipe [mg/kg]	APW analysis [mg/kg]
Na	281	6460	281.00	6460	6635
K	1.92	75.1	1.92	75.1	80.0
Ca	18.9	757.5	18.90	775.9	712.3
Mg	22.0	534.7	22.00	534.7	512.7
Sr	0.46	40.3	0.46	0	<10
Cl	327	11593	322.55	11595	11921
Br	0.55	43.9	5.00	399.5	415.8
SO_4	16.8	1614	16.80	1614	1600
TIC	3.89	237.3 (HCO_3)	3.89	0	<10
TOC		10.9		0	11.6
pH	7.0				6.54
$\delta^{18}O$ [‰ V-SMOW]					-11.21
$\delta^{2}H$ [‰ V-SMOW]					-81.2

*Vinsot et al. (2008) report data in units of mmol/L. Because water density at the salinity of the water is close to 1, the data can also be written in units of mmol/kg solution.

Table 3: Composition of the DGR APWs

	Estimate of pore-water composition			APW 1 (Br-poor)			APW 2 (Br-rich)		
	Original data [mmol/kg]	Original data [mg/kg]	Data provenance	APW recipe [mmol/kg]	APW recipe [mg/kg]	APW analysis [mg/kg]	APW recipe [mmol/kg]	APW recipe [mg/kg]	APW analysis [mg/kg]
Na	1661.2	38191	Squeezed water	830.61	19096	20119	830.61	19096	20227
K	97.19	3800	Guelph ground water	48.60	1900	1944	48.60	1900	1955
Ca	1197.6	48000	Aq. extraction	598.80	24000	23248	598.80	24000	23511
Mg	195.06	4741	Squeezed water	97.53	2371	2345	97.53	2371	2367
Sr	20.86	1828	Squeezed water	10.43	914	<100	10.43	914	<100
Cl	4559.4	161647	Squeezed water adjusted for charge balance	2279.7	80823	81150	2230.2	79067	81113
Br	26.07	2083	Squeezed water	13.03	1042	1051	62.58	5000	5271
SO_4	<2	<160	Squeezed water	0	0	<16	0	0	<16
$\delta^{18}O$ [‰ V-SMOW]						-11.32			-11.32
$\delta^{2}H$ [‰ V-SMOW]						-81.0			-81.0

First, NaCl, KCl and NaBr were added to 400 g deionized water while shaking and stirring. In a glovebox, $CaCl_2$ was dissolved in 300 g water, and $MgCl_2$ in 100 g water. Dry $CaCl_2$ and $MgCl_2$ chemicals were used as purchased, as previous experience indicated that further drying prior the preparation of the solutions was not necessary. Once dissolution was complete, the solutions were removed from the glovebox. The $MgCl_2$ solution was mixed with the Na-K-Cl-Br solution, and finally the $CaCl_2$ solution was added. Last, water was added to yield a total 1000 g of solution. No precipitates were identified in the final solution.

2.3 ANALYTICAL METHODS

The squeezing technique is described in detail in Mazurek et al. (2015). Chemical analyses were performed on a Metrohm ProfIC AnCat MCS IC system with automated 5µl and 50µl injection loops (more detail in Wersin et al. 2013). Dilutions were prepared gravimetrically, so the unit for all data is mg per kg solution.

The adapted isotope diffusive exchange (AIDE) protocols are detailed in de Haller et al. (2016). In order to adjust the water activity of the test waters to that of the pore water, the following salt solutions were used for test waters LAB (local tap water) and SSI (glacial melt water, see Section 8.1.3):

	Mont Terri sample		DGR samples		
	H2O [g]	NaCl [g]	H2O [g]	NaCl [g]	CaCl2 [g]
LAB	19.9204	0.4554	19.9398	1.1959	1.7343
SSI	19.9038	0.4507	19.9536	1.1973	1.7339
	Na [mg/kg solution]	Cl [mg/kg solution]	Na [mg/kg solution]	Ca [mg/kg solution]	Cl [mg/kg solution]
LAB	8792	13558	20571	27387	80166
SSI	8711	13432	20582	27363	80140

In contrast to de Haller et al. (2016), all solutions were analysed for their isotopic composition without prior removal of Ca via addition of NaF. Water isotopic analyses were performed by HydroIsotop (Schweitenkirchen, Germany) by Cavity Ring Down Spectroscopy (CRDS), see Mazurek et al. (2013). The effects of high salinity on water isotopic measurements using the CRDS technique were thoroughly tested by comparing data obtained on pure water and artificial salt solutions prepared from that water. While salt solutions require a frequent cleaning of the syringes, no effects on the isotope data were identified. Therefore, the treatment with NaF (as required for measurements by ion-ratio mass spectrometry) was not necessary. A Picarro L 2130-i instrument was used. Samples were by default measured 6 times in a row, injecting 1.6 µL of sample each time. The isotope values and the standard deviations were obtained from the last 4 injections. If deviations of > 0.2 ‰ for $\delta^{18}O$ and > 1.5 ‰ for $\delta^{2}H$ within these 4 measurements were identified, a memory effect caused by the formation of salt crusts in the vapourizer was assumed. The memory effect is due to the presence of small amounts of water from the previous sample remaining in the salt crust. By increasing temperature in the vapourizer from 110 °C (default) to 140 °C, complete water release was attained, thus

eliminating this issue. Memory effects can be readily identified by evolving (i.e., not constant) $\delta^{18}O$ and $\delta^{2}H$ values in the 6 injections performed for each sample. The higher temperature was used for the DGR samples. After 18 samples, or when the standard deviations of the injections exceeded the threshold values, the salt crusts were removed from the vapourizer and syringe, and the analyses were repeated. Samples with a volume < 500 µL were analysed using 0.1 mL micro inserts. For system calibration, four internal standards were used, bracketing the sample solutions.

3. DIFFUSION CELLS

3.1 DESIGN REQUIREMENTS AND DIMENSIONING OF DIFFUSION CELLS

Considering that the diffusion cells should be suited for different sample types (e.g. different swelling pressures and pore-water salinities) as well as for different sample dimensions, the cell design had to satisfy various criteria, such as:

- providing volumetric confinement of the rock sample over a range of confinement pressures, up to about 5 MPa, to prevent swelling and induced pore-space changes;
- having a large contact surface between the rock sample and the APW to facilitate efficient exchange between APW and the pore water;
- allowing retrieval of representative samples of the equilibrating solutions over time on either side of the rock sample while keeping the system as undisturbed as possible;
- minimizing the volume ratio of APW to pore water, in order to retain detectability and resolution of changes in the equilibrating solutions over time;
- allowing some flexibility in terms of APW reservoir volume to adjust APW / pore-water ratios;
- use of corrosion-resistant materials for the entire cell, as the use of waters with high salinities was planned; and
- allowing flexibility in terms of dimensions (maximum diameter, thickness) of the rock samples to be equilibrated (see next paragraph).

In order to estimate the time scales needed for diffusive equilibration between pore water and APW in the external reservoirs on both sides of each core slice, design calculations were performed using FLOTRAN (Lichtner 2004). Figure 3 shows calculated diffusion profiles for slices 1, 1.5 and 2 cm thick. The initial pore water is assumed to have a nominal concentration of 1, while the concentration in the APW is 0. A diffusion coefficient of 4.8E-12 m^2/s and an anion-accessible porosity of 0.08 were considered for Cl diffusion at Mont Terri (Nagra 2014). Figure 3 indicates that full equilibration takes about 8 days for a slice 1 cm thick and 64 days for 2 cm. Diffusion coefficients for the shales from southern Ontario are about 3–4 times lower (NEA 2018), which results in correspondingly longer equilibration times. Further, the calculation is only valid for unretarded species, while cation transport is more or less strongly retarded, which further extends equilibration times. On this basis, it was decided to cut core samples to slices about 1.5 cm thick – this is considered the best compromise between attaining short equilibration times and limiting the number of slices per sample to a manageable number.

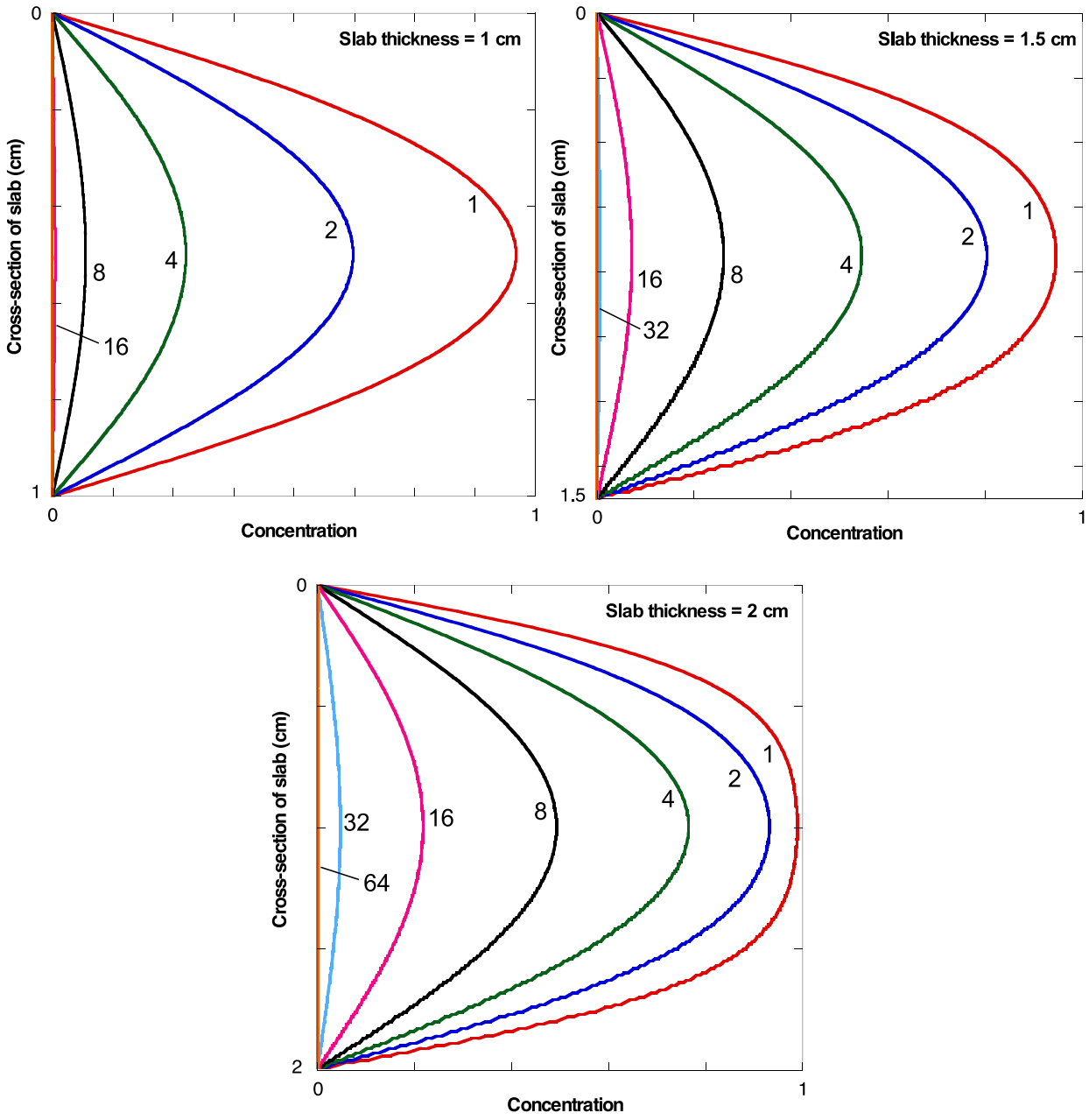

Notes: Numbers refer to time in days. Parameters used: D_e = 4.8E-12 m^2/s, porosity = 0.08.

Figure 3: Design Calculations for Diffusive Equilibration of a Solute of Initial Concentration 1 in Contact with Water of Concentration 0 on Both Sides of Slices 1, 1.5 and 2 cm Thick

3.2 PROTOTYPE DIFFUSION-CELL DESIGN

The diameters of the cores to be used for the experiments were 10.0 cm (Mont Terri) and 7.5 cm (DGR) with bedding perpendicular to the core axis. Therefore, diffusion cells were designed to be suited for drill core diameters of max. 10.0 cm, as this is also a common upper diameter limit for drill core samples taken for such purposes.

Based on the requirements identified in Section 3.1, a modular cell layout was designed around 2 square PETP plates containing a recessed, removable filter disc of sintered titanium, between which a rock slice of up to 4 cm thickness could be sandwiched (Figure 4). Multiple concentric cut-outs and borings within the PETP plate (Figure 5) allow for free circulation of APW between the filter disc and a detachable, transparent PMMA dome on the outer side of the PETP. Switching between domes with various cutout-depths allows for variable APW reservoir volumes. Two capillary ports, connecting to the cut-out volume in the PETP plate and the PMMA dome, are equipped with shut-off valves fitted with Luer-Slip ports to attach syringes for extracting and injecting solutions. Hydraulic sealing between the epoxy-embedded rock slice and the PETP plate containing the filter disc as well as between the PETP plate and the PMMA dome, is provided by NBR O-rings. The entire assembly is kept under axial confinement by two crosswise oriented clamping bars made from steel U profiles, with clamping force being controlled by the degree of deformation on a spring washer assembly. Technical detail on the different parts are given in Table 4.

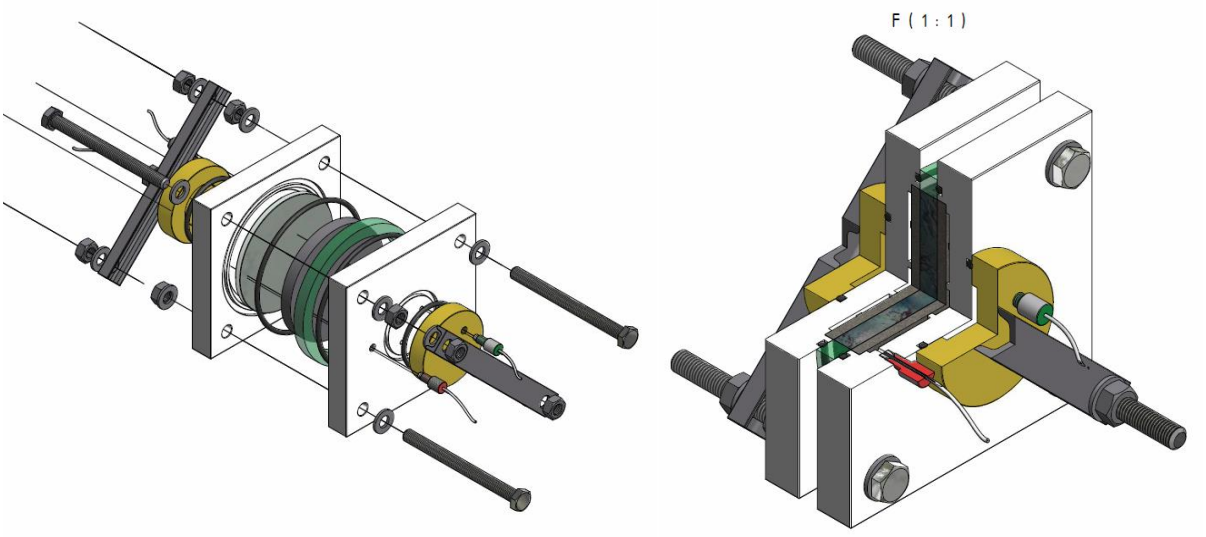

Notes: The PETP plates are shown in white, the PMMA dome in yellow, the sintered Ti filter discs in light grey, the rock slice as dark grey with green epoxy rim, O-rings in black. The sampling and injection capillary ports (red and green, respectively) are positioned apart from each other to prevent contamination of the equilibrated APW by the simultaneously injected fresh APW.

Figure 4: Exploded-view Drawing / 90° Section Cut of a Diffusion Cell

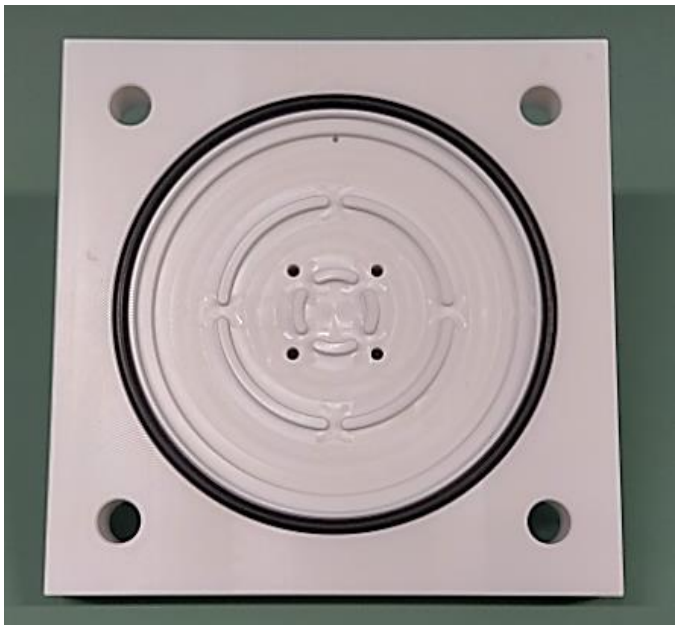

Notes: The concentric ridges have the same height as the rim along the edge of the cut-out and act as mechanical support for the inset Ti filter disc, which, in turn, is flush with the main PETP surface. The small hole at the 12 o'clock position of the cut-out is one of the two capillary ports. The black ring is the inset O-ring seal between the sample slice (which would be located in front) and the PETP plate.

Figure 5: Layout of the PETP Plate Cut-outs and Bores for APW Circulation

Table 4: Technical Details of the Principal Diffusion-cell Parts

Part description	Material	Dimensions
PETP plate	PETP (Ertalyte)	14 cm x 14 cm Prototype: 1.6 / 2 cm thick Experiment: 2 cm thick
Filter disc	porous sintered Ti, media grade 50 µm	10.0 cm diameter Prototype: 5 mm thick Main experiment: 3 mm thick
O-Rings	NBR-70	PMMA dome: 50.4 mm x 3.53 mm Sample/Plate: Prototype: 107.5 mm x 3.53 mm Experiment: 104.4 mm x 3.53 mm
APW reservoir dome	PMMA (transparent)	7.0 cm diameter, 1.5 cm thick
Capillary ports, tubing and luer-slip valves	Polyacetal, PTFE, HDPE, ETFE, PC, PP	capillary: 0.75 mm ID, 10 cm length
Clamping bars and bolting	Stainless steel (INOX A2)	Bars: 2 cm x 1 cm, 17 cm length Bolting: M10
Spring washer assembly	INOX 1.4310	

3.2.1 Design Aspect: Maintaining Volumetric Confinement

With the major swelling pressure in clay rocks being perpendicular to bedding, the radial (bedding parallel) confinement of the sample slices can be maintained by the stiffness of the epoxy and the PE tube. For the axial vector, maximum swelling pressures reported for Opalinus Clay reach up to 1.1 MPa (Giger & Marschall 2014). Counteracting these swelling pressures and maintaining isovolumetric confinement mandates that the filter plate does not deform. This requires either sufficient filter-plate support structures in the cut-out volume or sufficiently stiff filter plates to prevent deformation. As the first solution quickly leads to a more tortuous cut-out volume and a significant reduction of the interface surface between the APW and the filter disc, design efforts were focused on limiting such support structures and finding an optimized filter disc geometry that provides the required stiffness.

Filter disc deformation calculations

To estimate the required filter disc thickness, the maximum deflection in the centre of an unclamped, edge-supported circular disc under stress was calculated under an assumed maximum load of 5 MPa (providing an ample safety margin over the expected swelling pressure). Using the reported elastic modulus of the sintered Ti discs and an inner diameter of 2.2 cm for the unsupported part of the disc, a maximum deflection of 0.05 to 0.2 mm at its centre was calculated for disc thicknesses of 5 and 3 mm, respectively. At this stress, the sintered Ti discs also remain in the elastic deformation domain, and their deflection would be reversible after unloading. Based on these deliberations, a set of 5 mm thick filter discs were purchased for the prototype cells.

Filter disc deformation test

As the geometry of the unsupported disc surface between the support structures of the PETP plates is not simply circular, a deformation test was conducted on the 5 mm thick filter discs purchased for the prototype cells under a uniform 5 MPa load. For this, small spheres of plastically deforming, non-elastic modelling clay were positioned at various locations in the cut-out volume and covered by the filter disc. After loading the filter disc with 50 kg (roughly 0.06 MPa) the “initial” height of the modelling clay was measured with a micrometer gauge. Afterwards, the filter disc was loaded with 3800 kg (equivalent to 5 MPa) to simulate swelling. The resulting additional deformation on the modelling clay was measured between 0.08 to 0.13 mm for different locations (Figure 6). A measurement in the centre of the PETP plate (where the support geometry equals that used for the calculation of the edge-supported circular disc) gave a deformation of 0.06 mm, in agreement with the calculated value of 0.05 mm. As deflection decreases with proximity to a support ridge, only a minor part of the entire filter disc surface would suffer from maximum deflection. Therefore, the average deflection on the entire disc under these conditions is estimated to be below 0.03 mm for a 5 mm thick filter disc (which would scale to approximately 0.15 mm for a 3 mm thick disc based on the elastic moduli). Translating this into a potential swelling scenario of a 1.5 cm thick clay sample, the swelling-induced volume increase would be below 0.4 to 2 % for a 5 and 3 mm thick disc, respectively, even under these excessive swelling pressures.

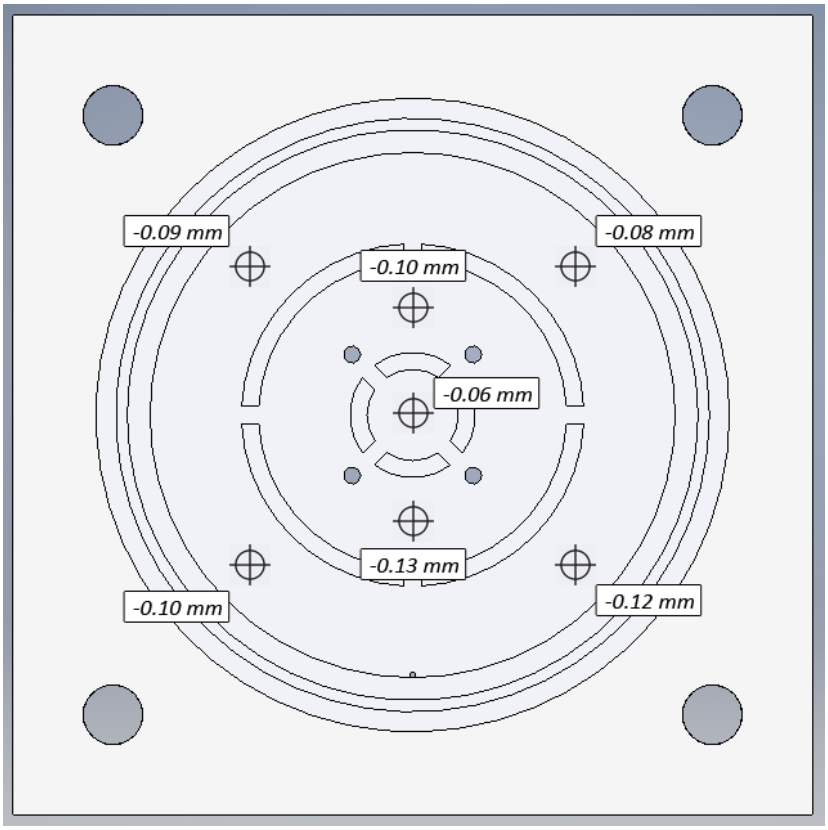

Notes: The indicated values reflect the measured reduction in height of the plastically deforming modelling clay pellets after increasing the load on the filter disc from 0.06 to 5 MPa. The systematically higher deformation in the lower part of the disc most likely represents a slightly distorted load distribution due to imperfect aligning of the piston of the hydraulic press used to apply the load.

Figure 6: Deformation of a 5-mm Thick Ti Filter Disc Under a Load of 5 MPa, Based on Experimentation

3.2.2 Design Aspect: Optimizing APW / Pore-water Ratio

In order to be able to observe and resolve small changes in the composition of the APW during equilibration, it would be desirable to have an APW / pore-water ratio close to 1. For the planned sample size of roughly 110 to 120 cm^3 of clay rock, and the porosities of the DGR and Mont Terri samples (8–20 vol.%, based on the gravimetric water contents listed in Table 1), this would translate into APW volumes between 4.4 and 12 mL per side of a diffusion cell. On the other hand, taking a sample to perform a chemical analysis of the current state of the equilibrating APW requires a minimum of 0.5 mL per side, with the extracted volume being replenished by fresh APW that still has the initial APW composition. As this replenishment causes a chemical disturbance of the system, the extracted/replenished volume should represent only a small fraction of the entire liquid volume in the cell.

Another important constraint on the APW volume in a cell is the high porosity (40–50 vol.%) of the filter discs. Individual maximum water contents for all filter discs were determined by saturating their pore volumes with distilled water under vacuum and weighing them in the dry

and water-saturated states. At a diameter of 10 cm, the maximum water contents are in the range 7.2–9.6 mL and 15.9–16.5 mL for 3 and 5 mm thick discs, respectively.

Optimizing the cell geometry within these constraints and requirements resulted in a design with the following water volumes (always as the sum of both sides):

Volume of PETP plate cut-outs and bores:	24.7 mL
PMMA dome volume:	5.8 mL
Filter discs (3 mm / 5 mm thickness)	18.0 / 32.4 mL *(average value)*
Total water volume per cell:	48.5 / 62.9 mL

As a result, sampling 0.5 mL per side leads to a recharge of the already equilibrated APW in the cell with roughly 2 vol.% of fresh, non-equilibrated APW, which should only marginally influence the APW composition in the cell. Attainable ratios of APW / pore water with this geometry for 3 mm thick filter discs (as used for the main experiment, see Section 3.3) are about 2.1 for Opalinus Clay samples and 5.3 for DGR samples.

3.3 A REVISION OF DIFFUSION-CELL DESIGN FOR MAIN EXPERIMENT

Based on observations and experience gained from the prototype experiment (Section 4), the design of the diffusion cells was improved for the main experiment in the following ways:

- *Thickness of the PETP baseplates:* based on a comparison of deformation measurements (amount of flexing of the plate along its diagonal) on the 16 and 20 mm thick prototype baseplates, a uniform thickness of 20 mm was adopted to improve mechanical rigidity.

- *O-ring seal between sample disc and baseplate:* in the prototype, the O-ring seal was situated very close to the contact between the epoxy resin and the PE tube. As this contact is mechanically weak due to low adherence between epoxy and PE, it could be a potential leakage point or a hydraulic pathway connecting the two sides of the cell. Therefore, the diameter of the O-ring was reduced, so that the seal lies entirely in the epoxy part of the disc.

- *Position of capillary port used for sampling:* the capillary port in the PETP baseplate of the prototype was slightly offset from the circumference of the cutout for the APW. This made it almost impossible to completely remove gas bubbles (e.g. air entrained during sample loading or intermittent APW sampling/recharging) from the APW during the experiment. Relocating this port to the circumference alleviated this problem.

- *Thickness of the sintered Ti filter disc:* based on the results of the deformation test performed on the 5 mm thick prototype filter discs (see Section 3.2.1), a filter disc thickness of 3 mm was selected for the main experiment. This allowed reduction of the APW content in the filter disc by over 40 %, while retaining sufficient mechanical rigidity to prevent swelling of the sample.

A series of 25 cells were then built based on these improved specifications. Additionally, a set of customized tools and support moulds were produced to facilitate sample loading and cell

assembly. This change effectively minimized sample exposure times to air during cell assembly (from ~15 minutes in the prototype experiment, to less than 5 minutes, with an average of 3 min, in the main experiment), decreasing the available time for samples to undergo desiccation and oxidation.

4. PROTOTYPE EXPERIMENT

An Opalinus Clay sample from Mont Terri (sample MT BDR-B7 8.54, adjacent and lithologically comparable to sample MT BDR-B7 9.45 listed in Table 1) was used for the prototype experiment. Three slices, each 1.1–1.4 cm thick, were prepared from the core. They were mounted in prototype diffusion cells and equilibrated with the Mont Terri type APW over a period of about 3000 h (125 d) at an ambient temperature of 20–22 °C. In slice 2, the evolution of the APW composition was monitored.

4.1 EVOLUTION OF APW COMPOSITION OVER THE EQUILIBRATION EXPERIMENT

The evolution of the APW composition over time is listed in Table 5 and shown graphically in Figure 7.

- For all solutes, no systematic differences are observed between sides A and B of the slice.
- Na and K contents are constant over time, and the last APW after an equilibration time of 2928 h is close to the value in the original APW. This correspondence indicates that the initial APW composition was close to that of the pore water, as intended.
- Similarly, Ca and Mg concentrations show no evolution over time. While Mg in the original and the last APW are near-identical, the Ca concentration in the last APW is 6.8 % below that in the original APW. This value is close to the analytical uncertainty of ±5 %.
- After a slight increase within the initial 500 h (21 d), Cl concentrations remain near-constant. It appears that the initial APW has a slightly lower Cl content than the pore water, and equilibrium is then attained at 500 h. This fits well with the design calculation shown in Figure 3 (slice thickness = 1.5 cm).
- Br concentration is constant over the entire experimental period and also fits well with the content in the initial APW. Only the first APW taken at an equilibration time of 72 h shows a slightly lower Br concentration. This is remarkable, given the fact that the pore water has a Br concentration around 40 mg/kg, and mixing of this water with the APW would be expected to yield an initial depression in the Br curve. However, let us note that the Br-accessible pore volume in the rock sample is about 11 mL (considering a Br-accessible porosity fraction of 0.6), i.e., much less than the volume of the APW (about 63 mL, see Section 3.2.2), so the dilution effect is only minor.
- SO_4 concentration increases slightly within the first 500 h, probably reflecting the fact that the pore water has a higher content than the initial APW. At late equilibration times, a weak decrease is seen, though it is within the analytical error of ±5 %.

Table 5: Prototype Sample MT BDR-B7 8.54, Slice 2 – Evolution of the Chemical Composition of the APW

Lab ID	Side	Time since loading [h]	Na [mg/kg]	K [mg/kg]	Ca [mg/kg]	Mg [mg/kg]	Cl [mg/kg]	Br [mg/kg]	NO3 [mg/kg]	SO4 [mg/kg]
APW original		0	6635	80.0	712.3	512.7	11921	415.8		1600
aPW-01A	A	72	6563	91.0	677.2	489.8	12381	395.8	<8	1784
aPW-02A	A	192	6782	94.4	676.7	510.0	12805	410.7	21.0	1799
aPW-03A	A	336	6733	90.6	673.7	506.6	12693	410.1	32.8	1788
aPW-04A	A	504	6976	93.6	681.7	521.9	13186	422.0	35.1	1813
aPW-05A	A	672	7028	93.1	685.1	527.8	13435	432.7	46.6	1844
aPW-06A	A	1008	6631	89.4	680.6	506.7	12675	414.9	8.9	1849
aPW-07A	A	1344	6611	88.9	670.7	502.3	12574	412.4	8.8	1843
aPW-08A	A	1728	6802	91.3	677.3	516.0	12907	424.8	33.5	1817
aPW-09A	A	2112	6755	89.7	671.0	511.2	12787	425.9	9.3	1823
aPW-10A	A	2544	6798	90.2	674.2	520.8	12979	428.2	<8	1808
aPW-11A	A	2928	6772	89.9	661.6	513.3	12795	424.9	<8	1787
aPW-01B	B	72	6446	76.4	667.5	500.3	12265	417.5	<8	1745
aPW-02B	B	192	6652	87.2	676.4	492.1	12730	417.1	9.8	1810
aPW-03B	B	336	6723	88.9	676.9	500.9	12825	416.9	<8	1826
aPW-04B	B	504	6798	93.3	681.3	510.0	13066	424.6	<8	1836
aPW-05B	B	672	6823	91.3	669.3	510.7	12883	421.3	<8	1810
aPW-06B	B	1008	6606	88.4	682.9	497.7	12679	414.7	50.6	1833
aPW-07B	B	1344	6582	89.2	678.5	499.1	12601	414.4	89.2	1824
aPW-08B	B	1728	6794	91.6	684.4	515.8	13101	430.1	23.0	1840
aPW-09B	B	2112	6878	92.4	675.1	520.6	13065	431.1	<8	1814
aPW-10B	B	2544	6746	91.5	673.2	519.7	12939	430.6	<8	1813
aPW-11B	B	2928	6779	89.9	666.0	516.1	12780	420.7	<8	1765

The following solutes were also quantified but are below detection for all samples: NH_4 <50 mg/kg, Sr <50 mg/kg, F <8 mg/kg.

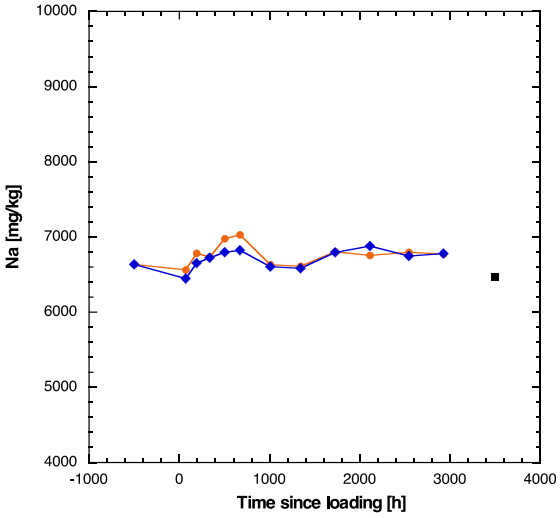
Na [mg/kg]
10000
9000
8000
7000
6000
5000
4000
-1000
0
1000
2000
3000
4000
Time since loading [h]

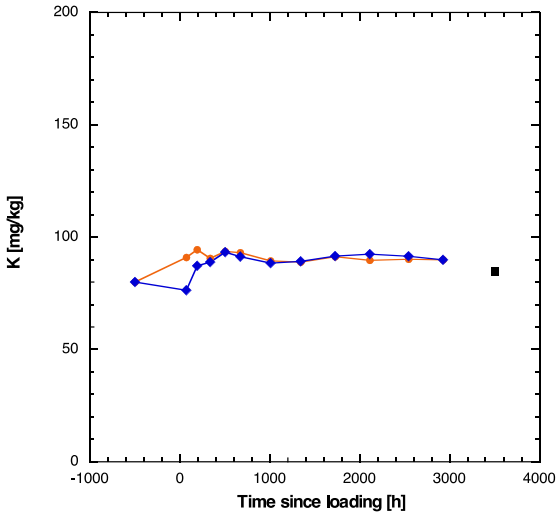
K [mg/kg]
200
150
100
50
0
-1000
0
1000
2000
3000
4000
Time since loading [h]

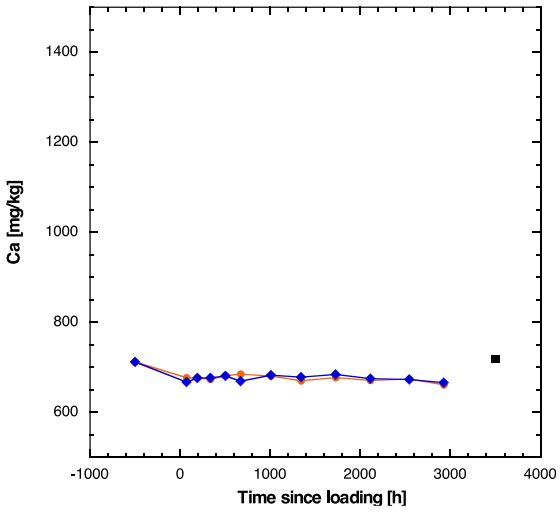
Ca [mg/kg]
1400
1200
1000
800
600
-1000
0
1000
2000
3000
4000
Time since loading [h]

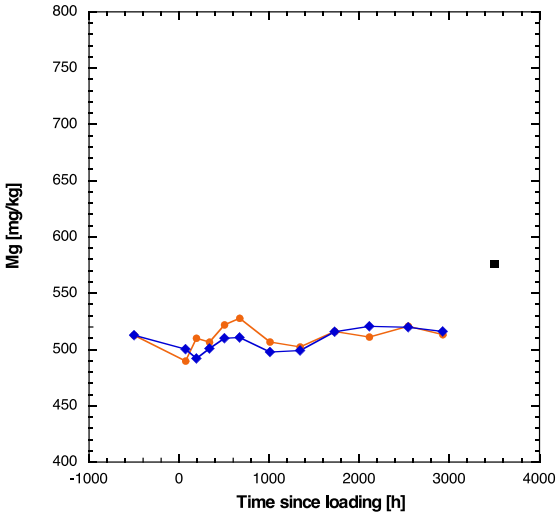
Mg [mg/kg]
800
750
700
650
600
550
500
450
400
-1000
0
1000
2000
3000
4000
Time since loading [h]

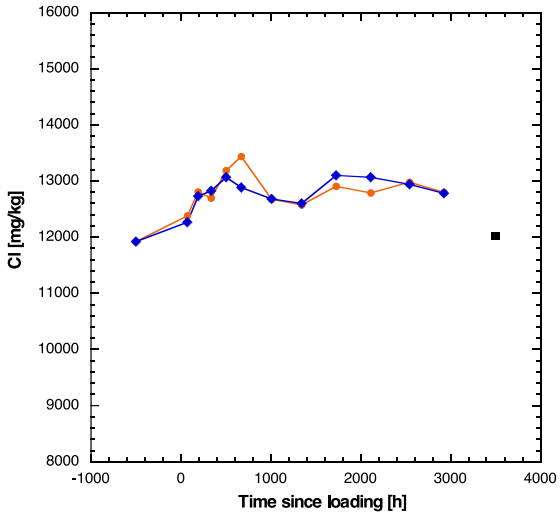
Cl [mg/kg]
16000
15000
14000
13000
12000
11000
10000
9000
8000
-1000
0
1000
2000
3000
4000
Time since loading [h]

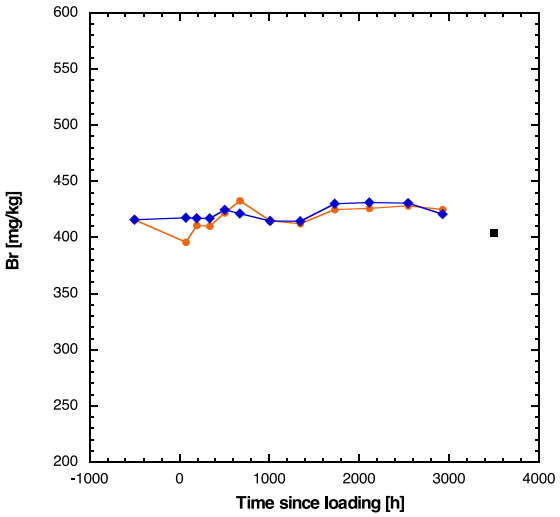
Br [mg/kg]
600
550
500
450
400
350
300
250
200
-1000
0
1000
2000
3000
4000
Time since loading [h]

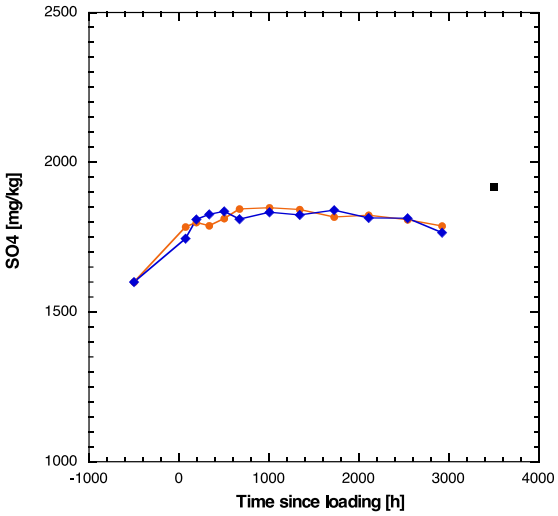

Notes: Point at -500 h: initial APW composition; point at 3500 h: composition of water squeezed at the lowest pressure. Orange and blue symbols: sides A and B of the diffusion cell.

Figure 7: Prototype Experiment (sample MT BDR-B7 8.54, slice 2) – Evolution of APW Composition with Equilibration Time, Including Comparison with the Original APW and the First Water Squeezed from the Sample after Termination of the Equilibration

4.2 COMPOSITION OF WATERS SQUEEZED FROM THE SAMPLE AFTER EQUILIBRATION

The 3 slices were re-assembled, vacuum-sealed into plastic bags and sent to CRIEPI (Japan) for pore-water squeezing. There, the material was rapidly hammered to cm-sized pieces within a plastic bag and then immediately inserted into the squeezing cell. Waters were obtained at pressures of 100 MPa, (5.92 g), 150 MPa (1.35 g), 200 MPa (1.02 g) and 500 MPa (3.28 g). The compositions of these waters are listed in Table 6. The data are also shown in Figure 7, together with the APWs of slice 2. As already known from previous studies (e.g. Mazurek et al. 2015), the concentrations of monovalent ions (Na, K, Cl, Br) decrease with pressure, likely due to ion filtration effects. On the other hand, bivalent cations (Ca, Mg) show an increase in concentrations with pressure, probably due to the dissolution of carbonate minerals.

In comparison to the last APW, the water squeezed at the lowest pressure (100 MPa) yields concentrations of Na, K, Cl and Br that are 4.5–6 % below those of the APW. On the other hand, concentrations of Ca and Mg are 8–12 % higher. These slight differences may be due to limited effects of ion filtration and pressure-dependent mineral solubility even in the first squeezed water. SO_4 content in the squeezed water is 8 % above that of the last APW, possibly due to a contribution from mineral oxidation during sample handling prior to squeezing. Overall, the results indicate that the deviation of the composition of the first squeezed water from the last APW is limited to the range of -4.5 to +11.9%.

Table 6: Prototype Sample MT BDR-B7 8.54 – Composition of Squeezed Waters

Squeezing pressure [MPa]	pH (lab)	Na [mg/kg]	K [mg/kg]	Ca [mg/kg]	Mg [mg/kg]	Sr [mg/kg]	F [mg/kg]	Cl [mg/kg]	Br [mg/kg]	NO3 [mg/kg]	SO4 [mg/kg]	TOC (direct) [mg/kg]	TIC (direct) [mg/kg]	Acetate [mg/kg]
100	8.40	6465	84.7	718.9	575.8	23.2	6.9	12025	403.7	3.3	1917	209.8	11.7	<10
150	7.88	5996	57.5	746.5	593.7	20.3	5.4	11200	386.3	2.0	1988	177.7	18.5	24.3
200	7.85	5918	45.4	752.1	590.6	20.4	4.9	10890	366.7	2.1	2013	171.5	19.5	12.9
500	8.38	3767	25.3	852.0	713.2	21.0	5.1	8230	272.6	1.5	1837	165.5	17.3	<10
				Deviation of squeezed water from last APW [%]										
		-4.6	-5.8	8.3	11.9			-6.0	-4.5		8.0			

Lactate, propionate and formate are <10 mg/kg in all samples.

5. MAIN EXPERIMENT: EQUILIBRATION OF SAMPLES WITH APW

The 4 cores used for the main experiment (Table 1) were dry cut to slices of about 1.5 cm thickness (Figure 8a). This resulted in a total of 23 slices (5 for the Mont Terri sample, 6 each for the DGR samples). These were subjected to diffusive equilibration (Figure 8b) over roughly 8 months at an ambient temperature of 20–22 °C. From all cells, 0.5 mL of the (partly equilibrated) APW was periodically extracted from both sides of the cells in syringes and was replaced by fresh APW (Figure 8c). One cell containing a Mont Terri slice (slice #1) had to be abandoned as it started to leak during the experiment.

5.1 EVOLUTION OF APW COMPOSITION OVER THE EQUILIBRATION EXPERIMENT

Time-series analyses were performed only for 1 slice of each sample (Table 7 to Table 10), while the water aliquots taken from the other slices were stored as a backup without being analysed. At the time of disassembly of the diffusion cells, a final analysis of the APW was obtained for all slices (shown in blue in Table 7 to Table 10). Figure 9 to Figure 12 show the time evolution graphically. Lines connecting the penultimate and final APW compositions refer to the slice used for the time series. Note that TOC and TIC could not be measured in the time series due to the limited sample volumes. However, data are available for the last APWs.

In a small number of the final slices, SO_4 and/or NO_3 contents are higher than in other slices of the same sample. These anomalies, often linked to higher Ca or K contents, are likely due to oxidation, i.e. the O-ring in the diffusion cell was not perfectly tight. These effects can be seen for slice 13, 20 and 22 (side A) and slice 19 (side B). Note that the other sides of these samples do not show any anomalies. This illustrates the fact that there are no hydraulic shortcuts between sides A and B of the diffusion cells.

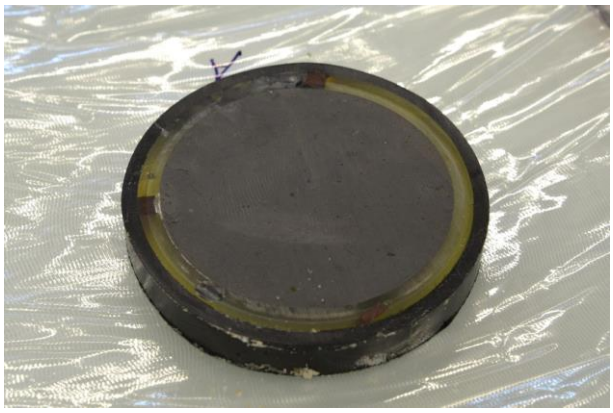

a

b

c

Figure 8: Illustration of Core Slices (a) and Equilibration Cells (b, c)

5.1.1 Opalinus Clay Sample

The same initial APW (with a Br tracer) was used on both sides of the rock slice, and the time evolution of the water was monitored only for side A. The match between the APW and the pore water appears to be good for most species, such that the compositions do not change substantially over time. Na, K, Ca and Cl contents show no time evolution at all, while Mg and SO_4 show slight increases. Br shows a more complex pattern with an initial decrease, followed by an increase at late times to values comparable to those of the initial APW. This evolution is not well understood. The pH of the APW stabilizes at a value of about 7.7.

Table 7: Sample MT BDR-B7 9.45 (Opalinus Clay) – Evolution of the Chemical Composition of the APW

Slice	Side	Time since loading [h]	Na [mg/kg]	NH4 [mg/kg]	K [mg/kg]	Ca [mg/kg]	Mg [mg/kg]	Sr [mg/kg]	Cl [mg/kg]	Br [mg/kg]	NO3 [mg/kg]	SO4 [mg/kg]	TOC [mg/kg]	TIC [mg/kg]
3	A	23.3	7194	<10	94.3	764.8	552.4	<10	12710	438.4	2.7	1733		
3	A	121.6	7236	<10	102.6	756.4	543.9	23.7	12713	409.8	2.9	1798		
3	A	161.7	7235	<10	99.9	753.1	548.5	26.8	12730	404.0	4.3	1822		
3	A	216.5	7159	<10	97.2	763.3	541.9	27.4	12602	394.7	3.3	1859		
3	A	264.1	7102	<10	96.7	747.3	539.9	28.8	12478	384.6	7.9	1799		
3	A	357.6	7123	<10	94.7	756.1	547.8	31.2	12693	388.2	2.6	1854		
3	A	597.2	7031	<10	94.2	752.6	549.1	32.0	12653	382.2	1.9	1881		
3	A	866.2	7137	<10	93.0	753.1	547.4	35.6	12538	376.8	2.0	1868		
3	A	1054	7146	<10	94.1	759.2	550.6	37.1	12566	379.9	4.1	1889		
3	A	1219	7035	<10	91.0	750.6	545.5	36.0	12500	377.1	1.8	1838		
3	A	1392	7041	<10	93.7	758.3	551.9	37.8	12644	379.7	2.3	1855		
3	A	1627	7062	<10	93.4	760.0	554.8	38.4	12651	385.2	3.2	1877		
3	A	1965	7021	<10	93.4	756.9	552.6	40.1	12547	381.7	2.3	1851		
3	A	2302	7111	<10	90.0	753.0	554.8	38.2	12538	381.8	1.9	1846		
3	A	6021	7093	<100	93.9	740.3	574.5	<100	12608	436.6	21.0	1946	1055	26.8
2	A	6021	7004	<100	83.8	762.1	556.1	<100	12462	429.9	21.7	1763	1121	16.8
4	A	6021	7017	<100	78.9	729.0	557.2	<100	12710	441.4	21.0	1802	998	17.4
5	A	6021	6958	<100	83.1	734.1	555.9	<100	12604	437.7	34.1	1769	1028	20.4
6	A	6021	7109	<100	82.3	767.4	575.8	<100	12820	442.4	29.1	1767	952	19.4

The evolution of the APW composition was monitored for slice 3. The final APW compositions were obtained for all slices and are shown in blue. Because the same initial APW was used on both sides of the diffusion cell, only waters from side A were analysed. The following solutes were also quantified but are below detection for all samples: NH_4 <10 mg/kg, F <1.6 mg/kg.

5.1.2 Queenston Formation Sample

As expected, solute concentrations in the original APW are lower than those in the pore water, leading to higher ion concentrations in the waters at the termination of the experiments. Na, K, Ca, Mg and Cl contents decrease initially but stabilize at late times, suggesting that equilibrium has been approached. SO_4 concentrations in the initially SO_4-free APW increase over the entire experimental period to levels that are substantially higher than in the other DGR samples (see below), which is due to the dissolution of small amounts of anhydrite (Table 1). Br contents on side A increase, while those on side B (Br-rich initial APW) decrease over the entire experimental period. The Br concentrations on both sides of the slices remain different (2856 mg/kg on side A, 4133 mg/kg on side B). The fact that Br did not equilibrate over the experimental period is due to: a) the low diffusive flux across the sample, and b) the fact that the total water volumes of the APWs on both sides exceed the total pore volume in the slices by a factor of about 5 to 6. Consequently, much longer equilibration times would be required to transport the Br inventory across the samples. For Br, a linear diffusion profile can be assumed for each slice, and the mean Br concentration in the pore water is closely approximated by the average values in the APWs on both sides.

5.1.3 Georgian Bay Formation Sample

Na, K and Ca remain essentially constant over the whole experiment, while Mg increases slightly. In contrast to the Queenston Formation sample, SO_4 remains low, without a clear trend. Br on side A (Br-poor APW) increases, while Br on side B (Br-rich APW) decreases to a similar extent as in the Queenston Formation sample, except in the slice that was used for the time-series measurements (highlighted by the connecting lines in Figure 11). In this slice, only marginal changes of Br concentration over time are identified, indicating that diffusive flux across this slice is lower than in the other slices in which the final Br concentrations on both sides converge to a similar degree as in the Queenston Formation sample. The likely explanation for this difference is lithological heterogeneity on the cm scale.

5.1.4 Blue Mountain Formation Sample

Na and Ca remain constant over time, within error, while K decreases slightly, in particular during the first part of the experiment. Mg and Cl increase until ~100–200 h and then remain relatively constant. Br increases on side A and decreases slightly on side B. As for the other DGR samples, Br is not equilibrated at the termination of the experiment. SO_4 shows a systematic increase over time but remains low in comparison with the Queenston Formation sample.

Table 8: Sample DGR-3 527.11 (Queenston Formation) – Evolution of the Chemical Composition of the APW

Slice	Side	Time since loading [h]	Na [mg/kg]	NH4 [mg/kg]	K [mg/kg]	Ca [mg/kg]	Mg [mg/kg]	Sr [mg/kg]	Cl [mg/kg]	Br [mg/kg]	NO3 [mg/kg]	SO4 [mg/kg]	TOC [mg/kg]	TIC [mg/kg]
11	A	76.9	23001	<100	2284	26848	2726	<100	93913	1282	158.2	23.5		
11	A	125.1	22838	<100	2227	26185	2673	<100	92262	1258	86.9	55.6		
11	A	166.3	23189	<100	2269	26609	2726	<100	94392	1287	228.8	109.9		
11	A	219.1	23172	<100	2260	26624	2742	<100	94652	1289	51.2	147.3		
11	A	267.6	23752	104.5	2301	27381	2835	148.7	96940	1328	106.3	196.4		
11	A	359.6	23641	114.8	2254	27466	2830	123.7	97360	1329	75.7	242.1		
11	A	602.9	23529	146.3	2214	27756	2823	128.3	96988	1412	92.4	409.2		
11	A	870.9	23125	155.8	2156	27485	2872	154.9	95903	1513	116.4	463.7		
11	A	1059	22665	170.2	2103	27061	2762	163.0	93774	1571	208.9	508.8		
11	A	1224	22739	149.9	2095	27115	2818	159.9	95223	1630	96.3	505.9		
11	A	1397	22512	148.1	2078	26867	2805	159.7	94884	1699	193.6	527.2		
11	A	1634	22503	135.7	2064	26846	2790	163.9	92365	1776	48.3	541.0		
11	A	1970	22420	137.0	2046	26861	2779	166.0	92348	1895	117.9	577.8		
11	A	2307	22169	128.6	2035	26557	2782	174.2	92277	2010	68.4	592.9		
11	A	6025	21922	<1000	2060	26106	2919	<1000	95424	2855	<160	668.7	552.8	7.55
7	A	6025	21977	<100	2040	26137	2875	<100	94244	2776	<16	664.9	674.5	4.75
8	A	6025	21519	<1000	2042	25522	2795	<1000	93565	2968	381.2	671.6	538.8	4.23
9	A	6025	21813	<1000	2017	26071	2908	<1000	95615	2809	<160	576.2	548.8	6.41
10	A	6025	21721	<1000	2012	25826	2891	<1000	95936	2963	<160	607.1	568.2	6.73
12	A	6025	21064	<1000	2030	24708	2728	<1000	91789	2610	<160	688.8	555.9	7.03
11	B	76.9	22374	<100	2182.1	25891	2653	<100	89903	5682	238.9	22.7		
11	B	125.1	23348	<100	2278.2	27034	2744	<100	93333	5719	93.2	55.6		
11	B	166.3	23895	<100	2314.4	27640	2831	<100	96745	5735	39.3	87.6		
11	B	219.1	23505	101.8	2264.8	27141	2769	<100	93367	5500	95.5	127.0		
11	B	267.6	23509	103.0	2248.3	27428	2782	109.3	96020	5475	35.8	145.2		
11	B	359.6	23452	110.1	2241.6	27547	2822	111.9	94437	5345	67.1	194.2		
11	B	602.9	23890	112.7	2262.8	28432	2948	144.2	98804	5276	69.9	367.1		
11	B	870.9	23019	129.1	2141.4	27743	2836	147.8	95540	4972	86.4	405.1		
11	B	1059	23249	127.2	2154.9	27940	2905	204.9	95583	4864	112.2	467.2		
11	B	1224	22642	124.9	2097.7	27299	2813	163.3	92000	4786	111.5	511.3		
11	B	1397	22705	162.8	2095.3	27292	2839	157.4	94408	4644	216.4	496.3		
11	B	1634	22574	129.7	2086.0	27126	2812	160.7	92925	4507	52.4	516.0		
11	B	1970	22123	143.6	2040.4	26620	2734	149.0	90884	4446	132.0	491.6		
11	B	2307	22082	129.4	2014.5	26688	2754	182.4	90539	4179	127.6	555.3		
11	B	6025	21854	<1000	2061.9	26132	2925	<1000	95336	4133	<160	690.3	547.9	6.83
7	B	6025	21711	<100	1987	25760	2736	137	86937	3314	336.6	638.2		
8	B	6025	21928	<100	2013	26046	2786	144	87199	3351	648.8	626.4		
9	B	6025	21865	<100	1982	25877	2774	145	88656	3106	111.1	599.5		
10	B	6025	22089	<100	1991	26093	2778	160	89004	3230	50.9	643.2		
12	B	6025	21335	<100	1975	25151	2683	117	85097	3981	174.3	709.8		

The evolution of the APW composition was monitored for slice 11. The final APW compositions were obtained for all slices and are shown in blue. Because the initial APW compositions on sides A and B differed (Br and Cl), both sides were studied. F was also quantified but is <16 mg/kg for all samples. Detection limits (e.g. for NH_4, Sr, NO_3) vary because different dilutions were used for IC analysis.

Table 9: Sample DGR-3 586.84 (Georgian Bay Formation) – Evolution of the Chemical Composition of the APW

Slice	Side	Time since loading [h]	Na [mg/kg]	NH4 [mg/kg]	K [mg/kg]	Ca [mg/kg]	Mg [mg/kg]	Sr [mg/kg]	Cl [mg/kg]	Br [mg/kg]	NO3 [mg/kg]	SO4 [mg/kg]	TOC [mg/kg]	TIC [mg/kg]
16	A	25.8	19876	<100	2029	22792	2423	<100	95921	1139	14.6	<16		
16	A	73.9	21033	<100	2046	24164	2483	<100	96673	1154	57.4	<16		
16	A	119.6	22857	<100	2142	26146	2618	<100	97291	1212	78.6	18.1		
16	A	160.4	22283	164.3	2090	25431	2600	<100	91071	1199	501.2	16.3		
16	A	214.2	23420	105.4	2122	26734	2676	93.8	95330	1240	42.0	17.9		
16	A	261.3	23226	103.6	2098	26319	2669	<100	93840	1238	98.2	30.6		
16	A	431.0	21269	117.6	1937	24198	2536	100.7	108789	1154	98.0	25.0		
16	A	550.9	21564	124.1	1951	24464	2598	157.8	103276	1189	68.3	23.9		
16	A	697.2	24032	120.5	2044	27593	2777	163.1	99152	1323	93.3	47.1		
16	A	835.1	23660	121.2	2045	27287	2782	184.4	98146	1315	69.5	36.5		
16	A	1006	23249	141.7	2013	26668	2813	192.8	105306	1259	17.0	26.0		
16	A	1198	23641	140.3	1983	27134	2796	188.3	101314	1263	23.5	29.9		
16	A	1488	23255	147.3	1931	26789	2764	187.4	95567	1252	24.1	27.7		
16	A	5397	22484	<1000	1957	25785	3093	<1000	98575	1506	<160	<160	641.2	6.43
13	A	5397	22795	<1000	2230	27543	2976	<1000	99616	2365	4550	314.7	492.9	4.93
14	A	5397	22503	<1000	1946	26071	2937	<1000	99057	2423	<160	<160	578.6	6.72
15	A	5397	22084	<1000	1940	25530	2941	<1000	96842	2688	<160	<160	533.0	5.49
17	A	5397	24570	<1000	1879	24706	2732	<1000	99034	2514	<160	<160	546.6	7.55
16	B	25.8	20790	<100	2116	24204	2562	<100	97561	4835	82.0	<16		
16	B	73.9	22223	<100	2137	25932	2586	<100	92210	5213	13.4	<16		
16	B	119.6	22368	<100	2108	25706	2585	<100	90405	5287	<16	<16		
16	B	160.4	22238	<100	2083	25637	2601	<100	89299	5179	21.1	<16		
16	B	214.2	22828	<100	2109	26239	2688	<100	91238	5291	<16	15.3		
16	B	261.3	22918	98.3	2110	26426	2677	114.6	90842	5299	<16	14.4		
16	B	328.3	22990	100.9	2093	26538	2695	168.5	90826	5253	18.0	17.1		
16	B	431.0	23052	119.3	2099	26634	2705	119.3	92653	5236	30.7	19.0		
16	B	550.9	22917	106.4	2034	26595	2695	152.9	91963	5162	<16	19.7		
16	B	697.2	23513	116.9	2082	27406	2786	144.1	93695	5305	17.2	21.8		
16	B	835.1	22552	113.3	2055	26467	2703	141.1	94846	5119	<16	27.9		
16	B	1006	22925	121.0	2014	26934	2741	133.6	90896	5169	<16	22.4		
16	B	1198	22582	120.0	1987	26311	2691	155.8	90186	5060	17.9	27.8		
16	B	1488	20730	113.2	1951	24238	2675	176.5	96526	4935	24.4	25.3		
16	B	5397	21822	<1000	2033	25159	2788	<1000	94188	5334	<160	<160	725.2	5.62
13	B	5397	22728	96.9	1959	26234	2802	177	89284	4054	467	68.8		
14	B	5397	22459	95.2	1923	25835	2807	213	89768	3777	36.8	68.3		
15	B	5397	21979	89.6	1843	25254	2711	182	88103	3578	69.0	57.3		
17	B	5397	23245	<100	1874	24833	2736	180	89493	3755	218	155		

The evolution of the APW composition was monitored for slice 16. The final APW compositions were obtained for all slices and are shown in blue. Because the initial APW compositions on sides A and B differed (Br and Cl), both sides were studied. Side A of slice 13 appears to have been affected by oxidation (high SO_4, NO_3, Ca, K, low TOC). F was also quantified but is <16 mg/kg for all samples. Detection limits (e.g. for NH_4, Sr, NO_3, SO_4) vary because different dilutions were used for IC analysis.

Table 10: Sample DGR-4 637.03 (Blue Mountain Formation) – Evolution of the Chemical Composition of the APW

Slice	Side	Time since loading [h]	Na [mg/kg]	NH4 [mg/kg]	K [mg/kg]	Ca [mg/kg]	Mg [mg/kg]	Sr [mg/kg]	Cl [mg/kg]	Br [mg/kg]	NO3 [mg/kg]	SO4 [mg/kg]	TOC [mg/kg]	TIC [mg/kg]
19	A	30.9	21799	<100	2119	25029	2548	<100	87911	1446	17.4	<16		
19	A	75.2	22570	<100	2100	25586	2575	<100	90189	1388	20.7	<16		
19	A	116.6	22164	<100	2075	25513	2584	<100	88606	1394	<16	<16		
19	A	170.2	22322	<100	2101	25651	2615	<100	90038	1406	13.7	19.2		
19	A	218.2	22836	<100	2093	26163	2657	117.2	92055	1427	22.0	21.1		
19	A	284.3	22846	<100	2088	26306	2680	101.2	92402	1411	<16	21.0		
19	A	390.4	23241	97.8	2080	26815	2699	121.4	93867	1411	30.8	31.7		
19	A	507.8	23670	104.5	2070	27308	2759	146.0	95386	1419	16.2	28.8		
19	A	654.1	23207	106.4	2016	26847	2734	149.6	93800	1399	<16	31.5		
19	A	792.0	23162	109.1	2001	26894	2755	162.3	93327	1408	96.5	46.0		
19	A	962.7	22924	115.1	1958	26749	2746	164.1	92966	1408	16.3	36.3		
19	A	1155	23281	117.6	1960	27188	2777	175.9	96317	1444	17.0	39.5		
19	A	1445	23184	120.2	1913	27257	2785	181.1	96185	1468	33.2	42.1		
19	A	5354	22107	<1000	1846	25818	2860	<1000	97397	2099	<160	<160	402.0	5.68
18	A	5354	21774	<1000	1815	25359	2864	<1000	96347	1906	<160	<160	359.0	7.74
20	A	5354	21862	<1000	1892	24955	2820	382.1	96163	1992	973.5	200.1	418.7	4.78
21	A	5354	22006	<1000	1855	25625	2886	<1000	97380	1973	181.0	<160	353.5	8.35
22	A	5354	21771	<1000	2117	26587	2817	<1000	96761	1935	4970	290.8	345.0	8.23
23	A	5354	21644	<1000	1892	25172	2801	<1000	96378	1964	<160	191.0	352.0	8.15
19	B	30.9	20573	<100	2111	23890	2547	223.8	93604	5538	30.8	<16		
19	B	75.2	22202	<100	2097	25757	2581	<100	92903	5399	27.5	<16		
19	B	116.6	22180	<100	2072	25695	2571	<100	89284	5391	83.9	41.5		
19	B	170.2	23188	<100	2150	26865	2690	<100	97788	5494	31.0	23.9		
19	B	218.2	23057	<100	2136	26731	2696	<100	92153	5499	19.1	23.7		
19	B	284.3	23213	<100	2124	26815	2711	106.7	92296	5466	16.3	24.4		
19	B	390.4	22632	93.6	2042	26161	2650	116.1	90183	5258	17.1	30.6		
19	B	507.8	23451	101.7	2076	27212	2759	123.5	93482	5385	<16	30.9		
19	B	654.1	22892	101.1	2006	26581	2707	138.1	90584	5228	<16	33.4		
19	B	792.0	22744	91.5	1983	26769	2723	128.3	94650	5316	<16	45.8		
19	B	962.7	22987	107.1	1975	26848	2750	140.4	91696	5195	14.4	39.6		
19	B	1155	22789	113.6	1927	26721	2735	159.6	91577	5106	<16	40.6		
19	B	1445	22840	121.5	1909	26923	2755	168.8	92275	5068	<16	45.6		
19	B	5354	22181	<1000	2156	27214	2878	<1000	96908	4997	5271	228.4	365.2	7.71
18	B	5354	21935	<100	1807	25228	2748	175	92621	4361	38.0	102		
20	B	5354	22189	<100	1854	25698	2702	138	87195	4282	215	156		
21	B	5354	22079	<100	1806	25543	2746	166	87803	4276	74.6	94.4		
22	B	5354	21493	<100	1787	24921	2674	152	87815	4435	72.0	84.6		
23	B	5354	21706	<100	1804	25102	2685	156	85392	4295	89.0	97.1		

The evolution of the APW composition was monitored for slice 19. The final APW compositions were obtained for all slices and are shown in blue. Because the initial APW compositions on sides A and B differed (Br and Cl), both sides were studied. Side A of slices 20 and 22, as well as side B of slice 19 appear to have been affected by oxidation (high SO_4, NO_3 ±Ca, K). F was also quantified but is <16 mg/kg for all samples. Detection limits (e.g. for NH_4, Sr, NO_3, SO_4) vary because different dilutions were used for IC analysis.

5.2 CONCLUSIONS

The fact that most ion concentrations remain constant over the whole experiment, or at least during the late stages, indicates a good equilibration between APW and pore water. Data obtained for different slices of the same core are consistent. Some of the slices show a limited degree of oxidation – highlighted by higher SO_4, Ca and K contents that do not fit the pattern of the other slices of the same core. These are nevertheless used to obtain the average composition of all slices of any sample, given the fact that all slices were re-assembled prior to squeezing. The Queenston Formation sample yields much more SO_4 than the other DGR samples, probably due to mineral dissolution. Br did not equilibrate in the DGR samples because it would take much longer times to transport the substantial mass of Br on the high-Br side across the sample. However, due to the symmetric changes in Br concentration of the two reservoirs, it is safe to assume a linear diffusion profile across the sample, so that the mean value of the final analyses on both sides can be considered to represent the mean Br content in the samples.

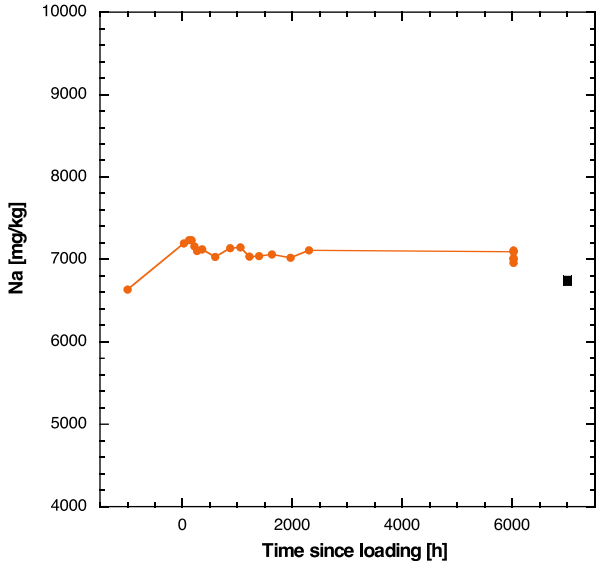
Na [mg/kg]
10000
9000
8000
7000
6000
5000
4000
0
2000
4000
6000
Time since loading [h]

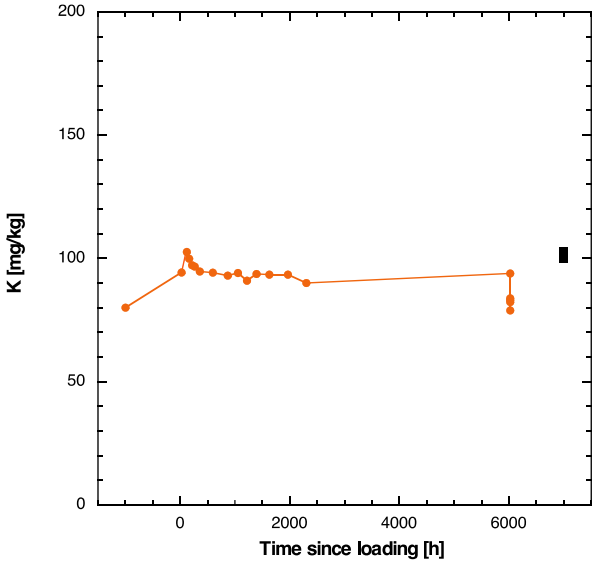
K [mg/kg]
200
150
100
50
0
0
2000
4000
6000
Time since loading [h]

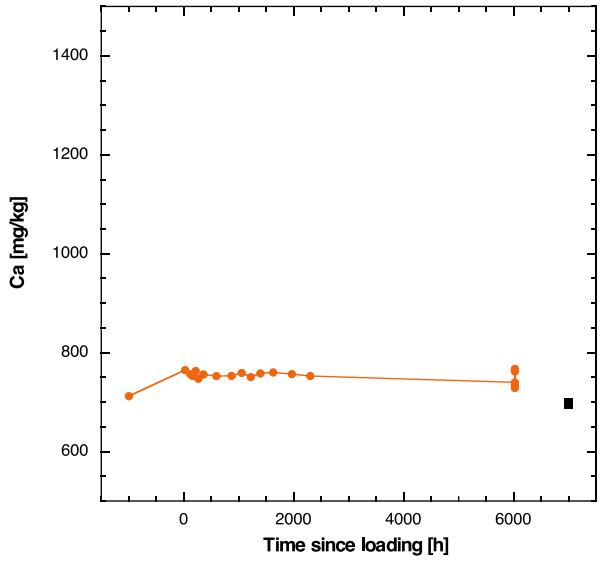
Ca [mg/kg]
1400
1200
1000
800
600
0
2000
4000
6000
Time since loading [h]

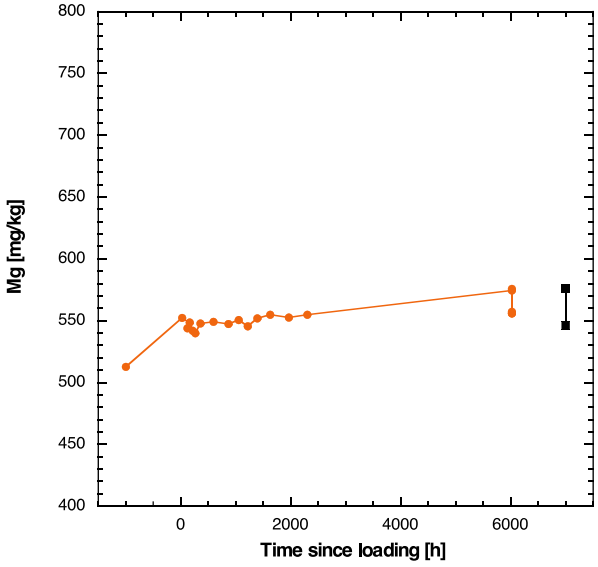
Mg [mg/kg]
800
750
700
650
600
550
500
450
400
0
2000
4000
6000
Time since loading [h]

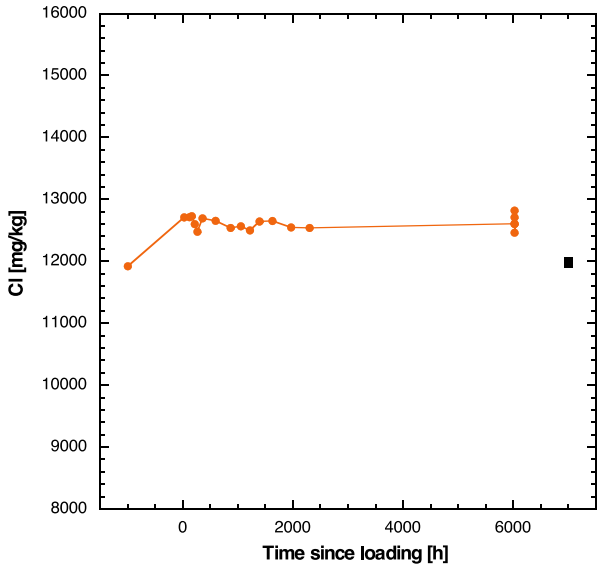
Cl [mg/kg]
16000
15000
14000
13000
12000
11000
10000
9000
8000
0
2000
4000
6000
Time since loading [h]

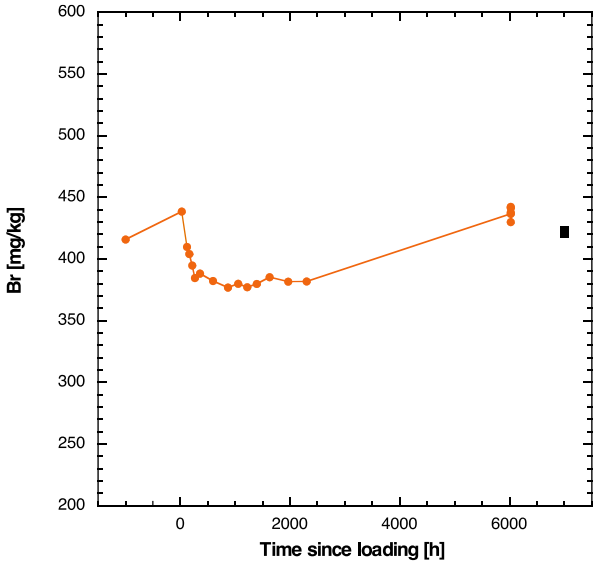
Br [mg/kg]
600
550
500
450
400
350
300
250
200
0
2000
4000
6000
Time since loading [h]

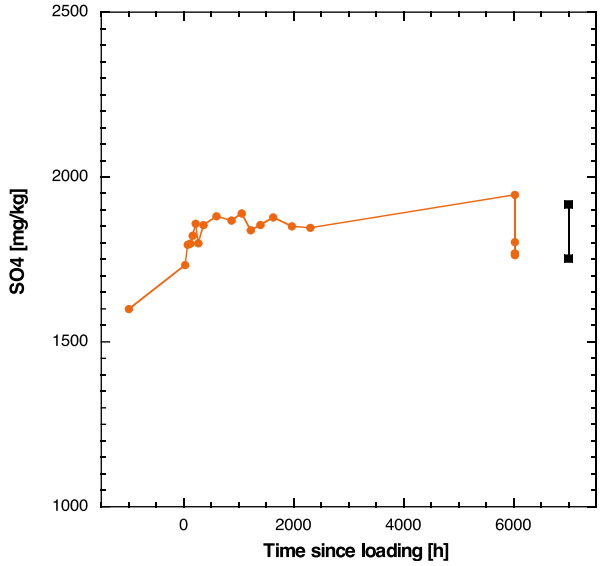

Notes: Point at -1000 h: initial APW composition; point at 7000 h: composition of water squeezed at the lowest pressure. Lines connecting the penultimate and final APW compositions refer to the slice used for time-series measurements.

Figure 9: Sample MT BDR-B7 9.45 (Opalinus Clay) – Evolution of the Chemical Composition of the APW

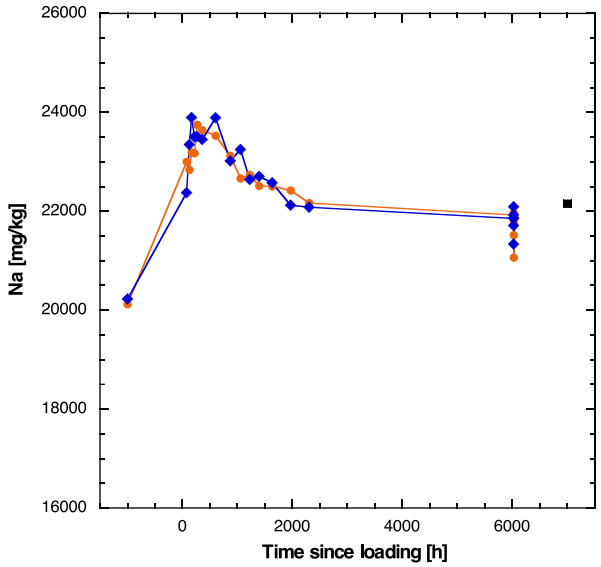
Na [mg/kg]
26000
24000
22000
20000
18000
16000
0
2000
4000
6000
Time since loading [h]

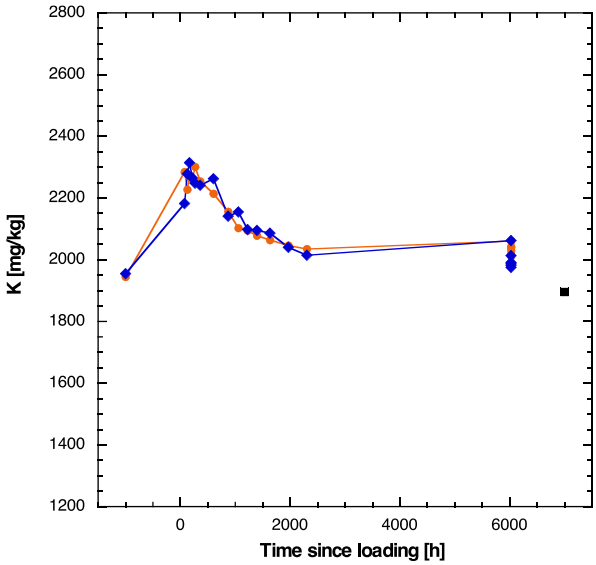
K [mg/kg]
2800
2600
2400
2200
2000
1800
1600
1400
1200
0
2000
4000
6000
Time since loading [h]

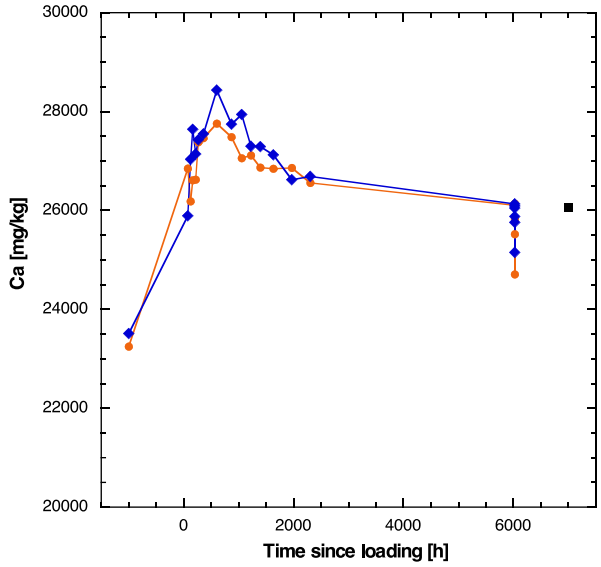
Ca [mg/kg]
30000
28000
26000
24000
22000
20000
0
2000
4000
6000
Time since loading [h]

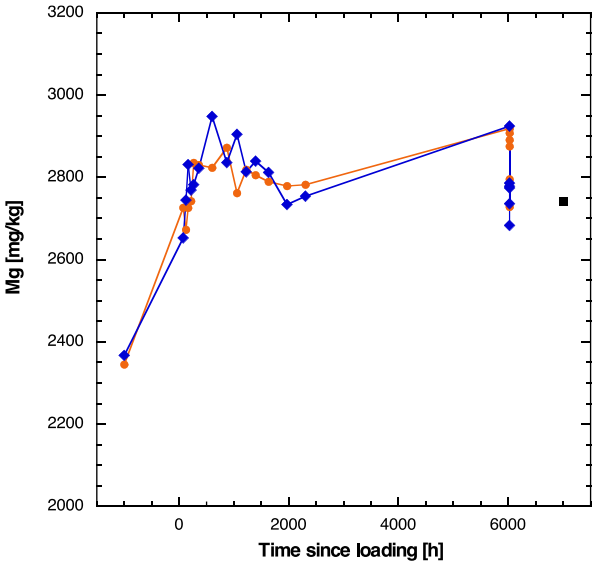
Mg [mg/kg]
3200
3000
2800
2600
2400
2200
2000
0
2000
4000
6000
Time since loading [h]

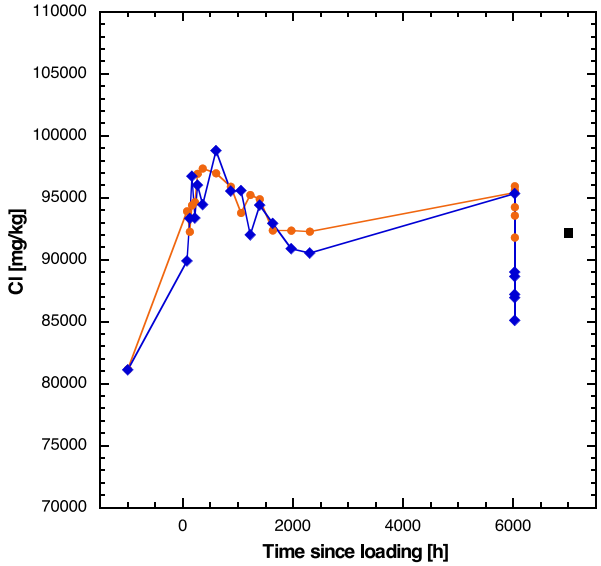
Cl [mg/kg]
110000
105000
100000
95000
90000
85000
80000
75000
70000
0
2000
4000
6000
Time since loading [h]

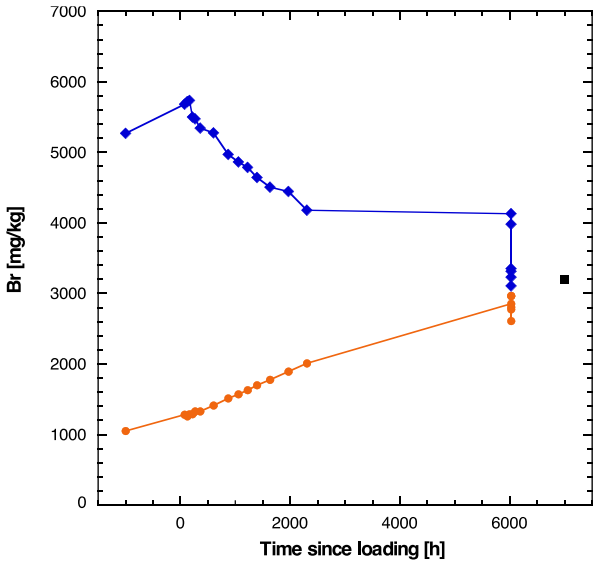
Br [mg/kg]
7000
6000
5000
4000
3000
2000
1000
0
0
2000
4000
6000
Time since loading [h]

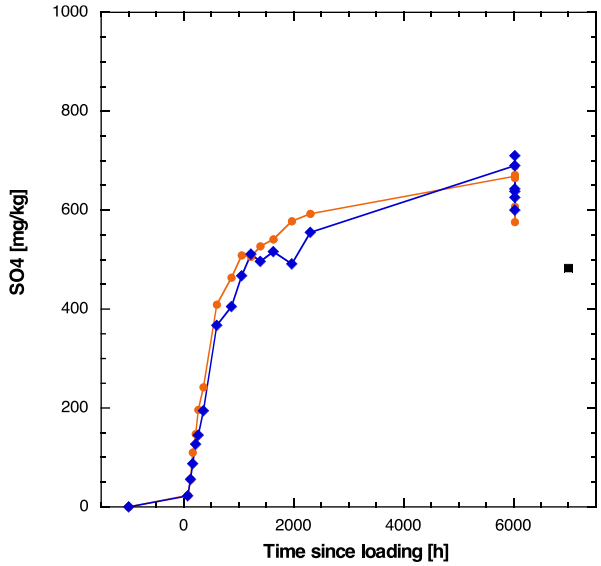

Notes: Point at -1000 h: initial APW composition; point at 7000 h: composition of water squeezed at the lowest pressure. Orange and blue symbols: sides A and B of the diffusion cell. Lines connecting the penultimate and final APW compositions refer to the slice used for time-series measurements.

Figure 10: DGR-3 527.11 (Queenston Formation) – Evolution of the Chemical Composition of the APW

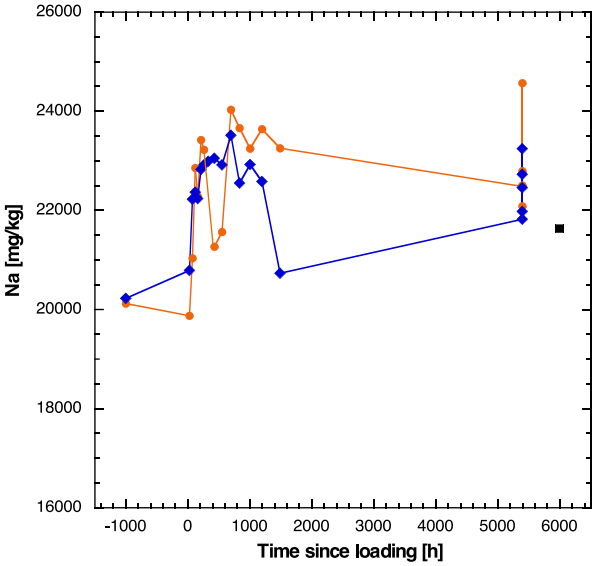
Na [mg/kg]
26000
24000
22000
20000
18000
16000
-1000
0
1000
2000
3000
4000
5000
6000
Time since loading [h]

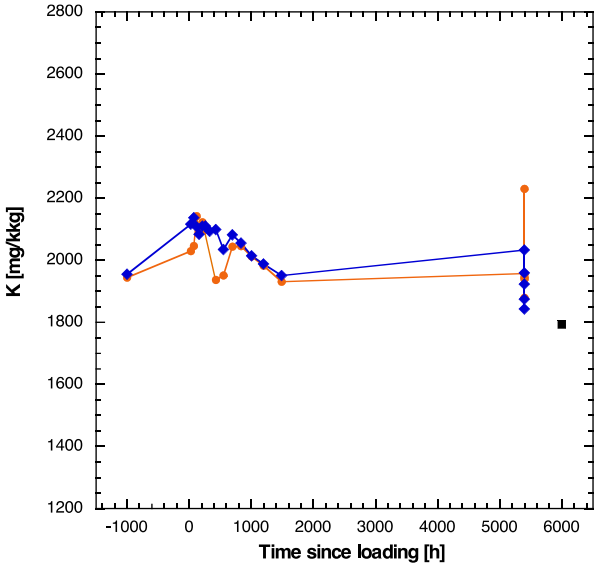
K [mg/kg]
2800
2600
2400
2200
2000
1800
1600
1400
1200
-1000
0
1000
2000
3000
4000
5000
6000
Time since loading [h]

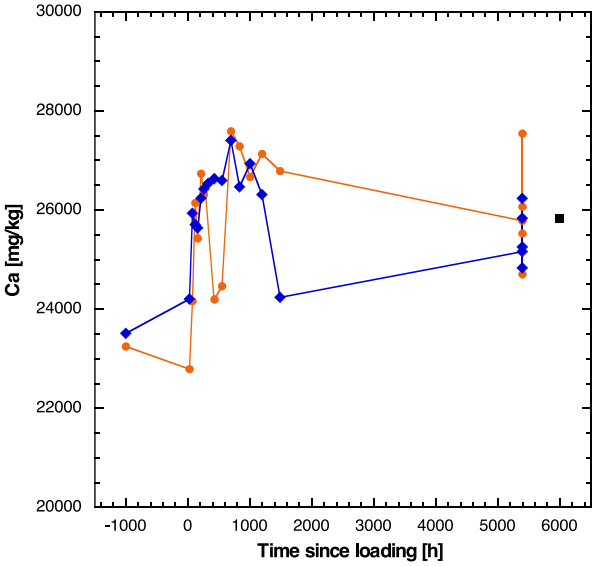
Ca [mg/kg]
30000
28000
26000
24000
22000
20000
-1000
0
1000
2000
3000
4000
5000
6000
Time since loading [h]

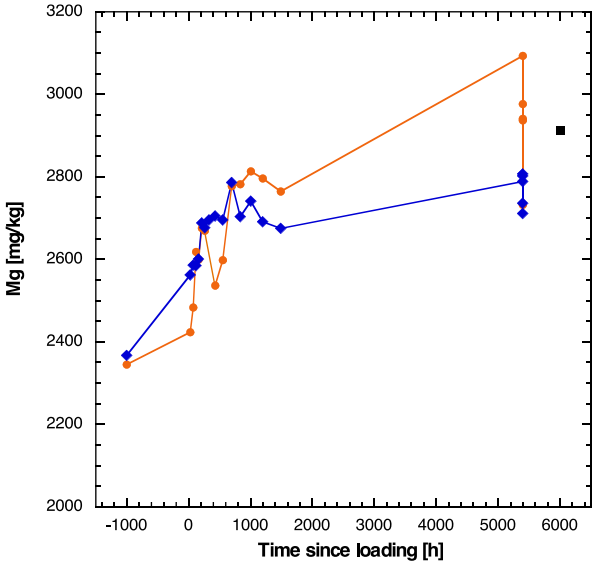
Mg [mg/kg]
3200
3000
2800
2600
2400
2200
2000
-1000
0
1000
2000
3000
4000
5000
6000
Time since loading [h]

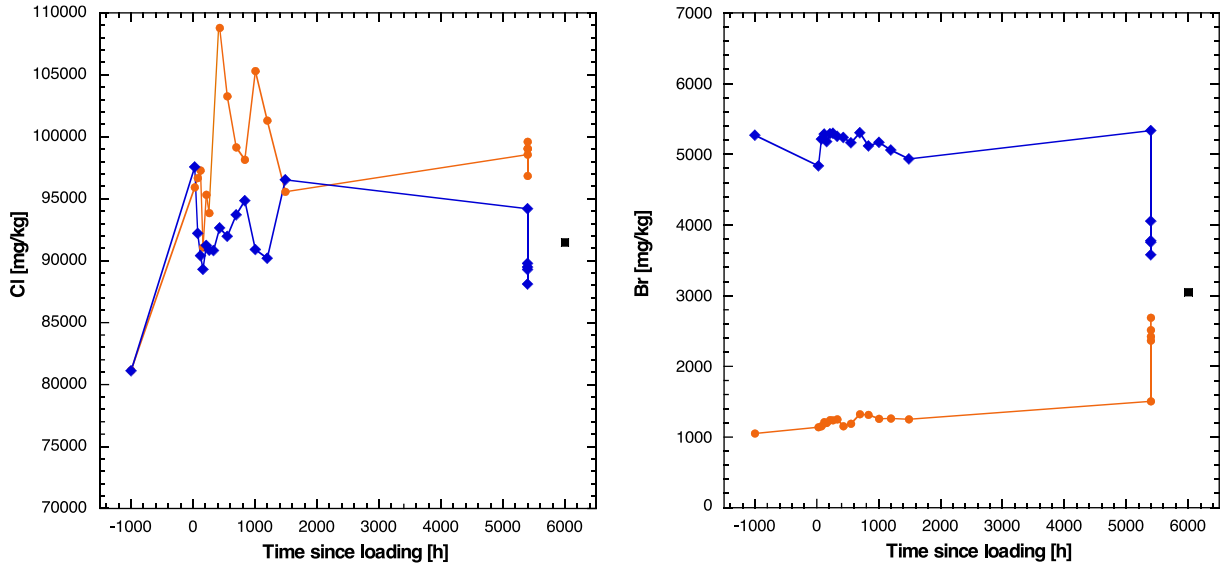

Notes: Point at -1000 h: initial APW composition; point at 6000 h: composition of water squeezed at the lowest pressure. Orange and blue symbols: sides A and B of the diffusion cell. Lines connecting the penultimate and final APW compositions refer to the slice used for time-series measurements.

Figure 11: Sample DGR-3 586.84 (Georgian Bay Formation) – Evolution of the Chemical Composition of the APW

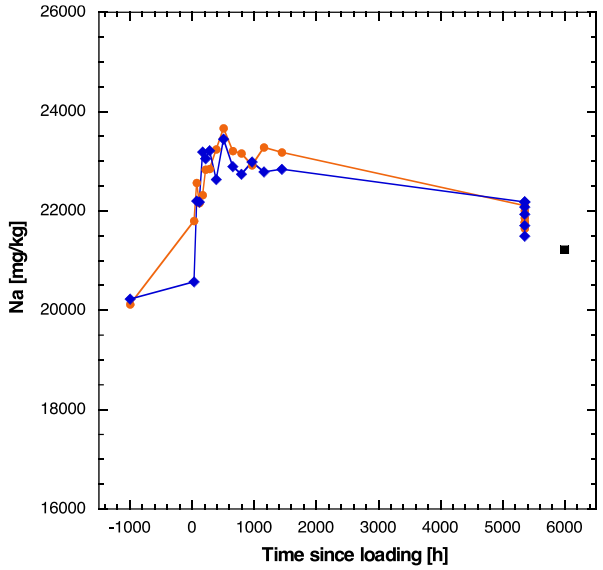
Na [mg/kg]
26000
24000
22000
20000
18000
16000
-1000
0
1000
2000
3000
4000
5000
6000
Time since loading [h]

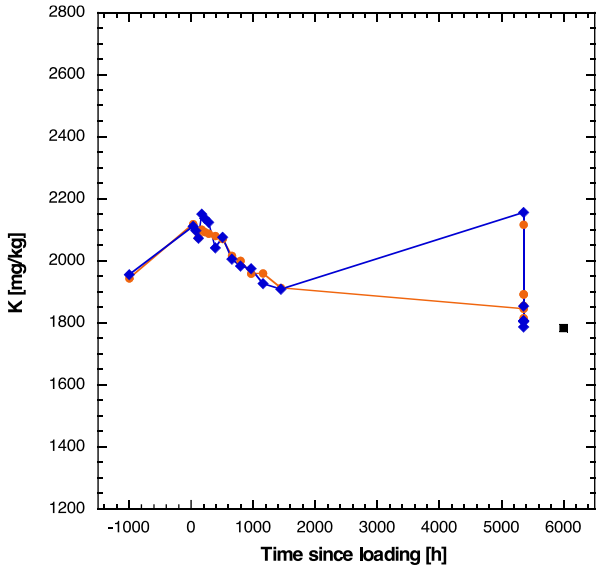
K [mg/kg]
2800
2600
2400
2200
2000
1800
1600
1400
1200
-1000
0
1000
2000
3000
4000
5000
6000
Time since loading [h]

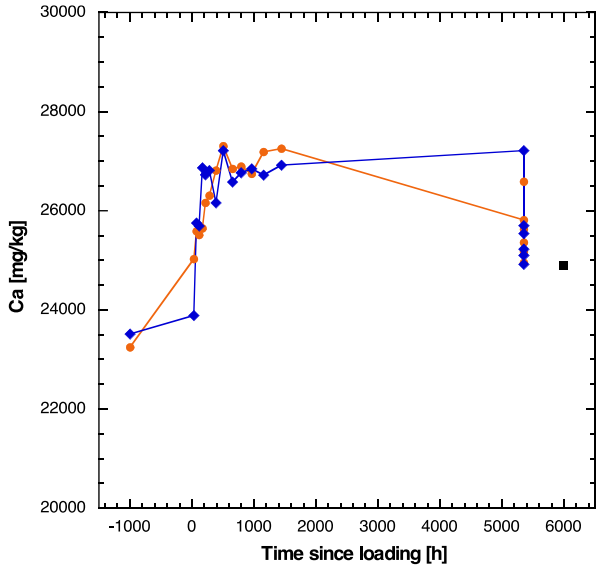
Ca [mg/kg]
30000
28000
26000
24000
22000
20000
-1000
0
1000
2000
3000
4000
5000
6000
Time since loading [h]

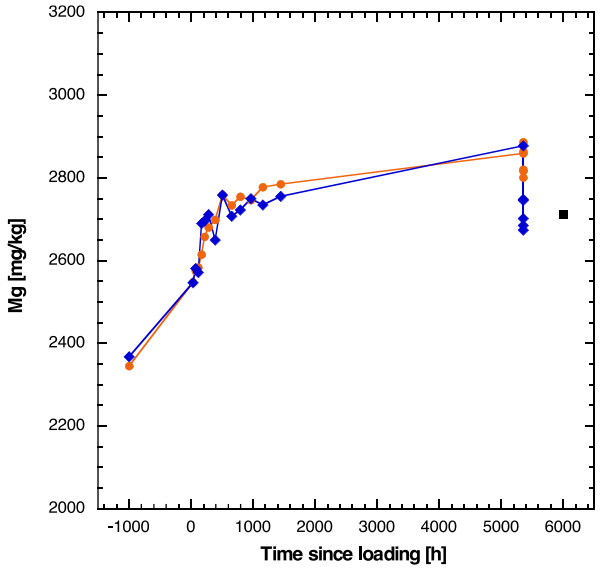
Mg [mg/kg]
3200
3000
2800
2600
2400
2200
2000
-1000
0
1000
2000
3000
4000
5000
6000
Time since loading [h]

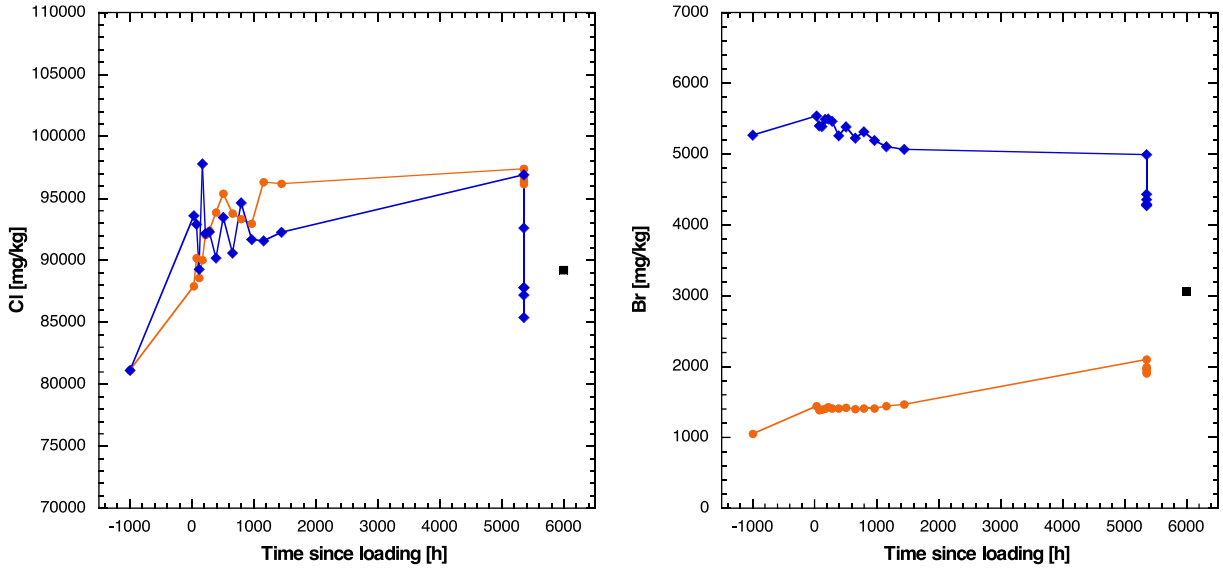

Notes: Point at -1000 h: initial APW composition; point at 6000 h: composition of water squeezed at the lowest pressure. Orange and blue symbols: sides A and B of the diffusion cell. Lines connecting the penultimate and final APW compositions refer to the slice used for time-series measurements.

Figure 12: Sample DGR-4 637.03 (Blue Mountain Formation) – Evolution of the Chemical Composition of the APW

6. MAIN EXPERIMENT: SQUEEZING OF EQUILIBRATED SAMPLES

6.1 PREPARATION OF SAMPLES FOR SQUEEZING

After extraction of the last APW aliquot, the equilibration cells were disassembled (Figure 13a,b), and the sample slices were immediately sealed into evacuated plastic bags (Figure 13c). For each drill core sample, one slice was additionally vacuum-sealed into Al-coated plastic and put aside for AIDE experiments (Section 8.1.3) following the standard protocols described in de Haller et al. (2016).

For all other slices the rock material was separated from the PE tube and the epoxy ring by dry cutting (Figure 13d) and peeling off the latter. Each rock slice was then immediately vacuum-sealed again. After disassembly of all cells, all rock slices from the same drill core (4 slices to 5 slices each) were reassembled and machined on a lathe to the final core diameter of 49 mm (Figure 13e) required for squeezing. These sample stacks were first vacuum-sealed in plastic (Figure 13f) and then again in a second layer of Al-coated plastic. These cores were subsequently sent to CRIEPI (Japan) for squeezing tests.

Figure 13: Disassembly of the Equilibration Cells and Sample Conditioning – Disassembling the Cell (a, b); Vacuum Sealing of the Slices (c); Dry Cutting of PE Tube and Epoxy (d); Machining of Reassembled Core (4-5 slices) to a Diameter of 50 mm (e); and Sealed Sample Ready for Squeezing Test (f)

6.2 RESULTS OF SQUEEZING TESTS

6.2.1 Squeezing Yield

Water was obtained from all samples, and the recovered masses are listed in Table 11. As expected, the Mont Terri sample yielded the largest amount of water. The relatively clay-rich samples from the Georgian Bay and Blue Mountain Formations produced first waters at 200 MPa, while the clay-poor sample from the Queenston Formation yielded a small mass of water only at 300 MPa and higher.

Table 11: Water Yield of Squeezing Experiments

Sample ID	Unit	Water squeezed at 50 MPa [g]	Water squeezed at 100 MPa [g]	Water squeezed at 200 MPa [g]	Water squeezed at 300 MPa [g]	Water squeezed at 400 MPa [g]	Water squeezed at 500 MPa [g]	Total water squeezed [g]
BDR-B7-9.45	Opalinus Clay	6.6	2.18	2.53	1.51	1.42	1.04	15.28
DGR-3-527.11	Queenston Fm.	-	-	-	0.34	0.38	0.36	1.08
DGR-3-586.84	Georgian Bay Fm.	-	-	2.37	0.94	0.67	0.64	4.62
DGR-4-637.03	Blue Mountain Fm.	-	-	0.73	0.93	0.90	0.73	3.29

6.2.2 Chemical Composition of Squeezed Waters

The chemical composition of squeezed waters is listed in Table 12. The Mont Terri and DGR samples show distinct evolution of water composition with squeezing pressure:

- For the Mont Terri sample, concentrations of monovalent ions (Na, Cl, Br) decrease substantially with pressure and may reach around 50 % of the value obtained at the lowest pressure. At the sample time, bivalent cations (Ca, Mg) show increasing values. Both these trends are consistent with existing evidence from the Opalinus Clay and are explained by effects of ion filtration and pressure-dependent mineral solubilities (Mazurek et al. 2015).

- The evolution with pressure is much weaker for the DGR samples. The strongest effect is seen for K, which decreases substantially for the Georgian Bay and Blue Mountain shale samples. A slight decrease, is observed for the clay-poor Queenston shale sample. The other monovalent ions (Na, C, Br) decrease only marginally or remain constant for all samples. Bivalent cations do not show any evolution with pressure.

Table 12: Chemical and Isotopic Composition of Squeezed Waters

Sample	Squeezing pressure [MPa]	pH (lab)	Na [mg/kg]	NH4 [mg/kg]	K [mg/kg]	Ca [mg/kg]	Mg [mg/kg]	Sr IC [mg/kg]	F [mg/kg]	Cl [mg/kg]	Br [mg/kg]	NO3 [mg/kg]	SO4 [mg/kg]	TOC [mg/kg]	TIC[mg/kg]
BDR-B7-9.45 upper	50	7.68	6751	<100	102.6	694.8	575.8	<100	<16	11965	422.8	42.1	1917	965.4	23.6
BDR-B7-9.45 lower	50	7.90	6730	<100	<100	698.6	545.9	<100	<16	12004	420.6	32.4	1753	962.8	20.1
BDR-B7-9.45	100	8.12	6064	<100	<100	805.6	549.0	<100	<16	10811	336.1	478.7	1873	922.8	20.6
BDR-B7-9.45	200	8.20	5170	<100	<100	722.8	599.6	<100	<16	9713	295.8	33.3	1898	891.2	19.3
BDR-B7-9.45	300	8.27	4408	<100	<100	800.3	659.5	<100	<16	8774	265.4	33.4	1904	863.8	27.3
BDR-B7-9.45	400	8.31	3632	<100	<100	854.8	728.3	<100	<16	7902	235.7	16.2	1873	837.7	26.7
BDR-B7-9.45	500	8.34	3380	<100	<100	908.9	772.8	<100	<16	7717	230.5	25.4	1906	793.0	21.9
DGR-3-527.11	300	7.53	22154	<1000	1896	26057	2741	<1000	<160	92166	3197	455.3	483.2		
DGR-3-527.11	400	7.76	21846	<1000	1923	26315	2908	<1000	<160	92549	3150	<160	557.5		
DGR-3-527.11	500		21549	<1000	1772	26153	2731	<1000	<160	91750	3142	<160	548.1		
DGR-3-586.84	200	7.45	21636	<1000	1793	25832	2913	<1000	<160	91478	3049	172.9	<160	833.2	19.4
DGR-3-586.84	300	7.46	20721	<1000	1317	25684	2781	<1000	<160	90361	3011	<160	<160	756.7	12.9
DGR-3-586.84	400	7.57	20146	<1000	1068	25952	2830	<1000	<160	89913	2939	155.2	<160		
DGR-3-586.84	500	7.36	19555	<1000	<1000	25911	2825	<1000	<160	88034	2853	266.0	<160		
DGR-4-637.03	200	7.19	21218	<1000	1783	24903	2711	<1000	<160	89230	3057	<160	<160		
DGR-4-637.03	300	7.39	20746	<1000	1615	25297	2670	<1000	<160	88848	3083	137.6	<160		
DGR-4-637.03	400	7.40	20221	<1000	1352	25070	2658	<1000	<160	88856	3096	<160	<160		
DGR-4-637.03	500	7.39	19244	<1000	1134	24731	2561	<1000	<160	85910	2991	<160	<160		

Due to the substantial mass of water squeezed from sample BDR-B7 9.45 at 50 MPa, waters obtained on the upper and lower outlets of the squeezing chamber were stored and analysed separately. For all other samples, waters obtained on both outlets were merged in a single water vessel.

6.2.3 Chemical Composition of Aqueous Extracts of Squeezed Cores

Squeezed rock samples were subjected to aqueous extraction at a solid/liquid mass ratio of 1. The main objective was to quantify the Cl and Br inventories, but analyses were nevertheless made for all major ions (Table 13). All extractions were performed in duplicate (a, b in Table 13).

Table 13: Chemical Composition of Aqueous Extracts of Squeezed Cores

Sample		pH (lab)	Na [mg/kg]	NH4 [mg/kg]	K [mg/kg]	Ca [mg/kg]	Mg [mg/kg]	Sr IC [mg/kg]	F [mg/kg]	Cl [mg/kg]	Br [mg/kg]	NO3 [mg/kg]	SO4 [mg/kg]	TOC [mg/kg]	TIC [mg/kg]	Total alkalinity (titration) [meq/L]	Lactate [mg/kg]	Acetate [mg/kg]	Propionate [mg/kg]	Formate [mg/kg]
BDR-B7-9.45	a	8.77	370.9	2.1	17.0	2.1	1.3	<1	6.8	187	5.6	1.4	395.5	57.6	44.1	3.63	<2	2.2	<2	<2
BDR-B7-9.45	b	8.73	371.1	<1	17.2	<1	1.4	<1	6.8	191	5.7	2.0	396.4	57.7	45.1	3.61	<2	2.3	<2	<2
DGR-3-527.11	a	7.78	883.7	10.5	419.7	1171	89.5	6.6	1.6	2898	92.5	3.1	1780	27.0	3.4	0.65	<20	<20	<20	<20
DGR-3-527.11	b	7.74	834.3	10.0	404.5	1145	83.2	6.1	<1.6	2651	86.0	<1.6	1784	24.7	3.5	0.59	<20	48.9	<20	42.6
DGR-3-586.84	a	7.75	853.6	13.8	423.4	340.2	34.2	3.2	<1.6	2271	67.7	2.8	98.6	51.9	3.5	0.59	<20	<20	<20	<20
DGR-3-586.84	b	7.88	801.7	12.3	390.6	339.6	37.3	3.1	<1.6	2309	74.1	<1.6	112.8	47.4	3.4	0.54	<20	<20	<20	<20
DGR-4-637.03	a	7.16	659.2	10.2	311.0	253.7	35.6	2.1	<1.6	1718	57.2	<1.6	280.0	34.6	11.4	1.13	<20	<20	<20	<20
DGR-4-637.03	b	7.51	650.5	9.8	292.3	249.1	35.0	2.2	<1.6	1721	55.8	6.8	216.2	31.6	11.2	1.06	<20	<20	<20	<20

6.2.4 Saturation Indices

In order to explore the potential control of SO_4 in the various water types by sulphate minerals, saturation indices for gypsum and anhydrite were calculated using the PHREEQC version 3 code (Parkhurst & Appelo 2013). For squeezed waters and APWs from DGR samples, the Pitzer data base (included in Parkhurst & Appelo 2013) was used, given the high salinity of the fluids. For the Mont Terri sample and for all aqueous extracts, the Thermochimie E-D 9b data base (Giffaut et al. 2014) was applied. Because Sr concentrations were below detection in most samples, saturation indices for celestite could not be calculated. In squeezed waters and APWs from samples DGR-3 586.84 and DGR-4 637.03, SO_4 concentrations were often below detection, such that saturation indices are available only for a few waters. Results are listed in Table 14.

- All waters of the Opalinus Clay sample BDR-B7 9.45, the Georgian Bay Fm. sample DGR-3 586.84 and the Blue Mountain Fm. sample DGR-4 637.03 are undersaturated with respect to gypsum and anhydrite, suggesting the absence of these minerals from the rock. No sulphate minerals were identified by XRD analysis (Table 1).

- All waters from the Queenston Fm. sample DGR-3 527.11 are close to gypsum saturation, even the aqueous extracts. This is consistent with the identification of trace amounts of anhydrite by XRD (Table 1). In this sample, SO_4 in all solutions is controlled by solid sulphate.

6.2.5 Water, Cl and Br Budgets, Anion-accessible Porosity

In clay rocks containing a negative structural charge, anions are affected by ion exclusion and, thus, only “see” part of the total porosity (e.g. Pearson et al. 2003). The anion-accessible porosity fraction can be derived from analysis of unreactive chloride or bromide by different methods, all of which are subject to some uncertainty. Here, chloride and bromide data obtained from squeezing and subsequent aqueous extraction of the squeezed samples are evaluated. The total mass of water in each sample can be obtained from squeezing and subsequent drying at 105 °C (Table 15). The total masses of Cl and Br in the samples can be calculated by adding the respective masses in squeezed waters and in aqueous extracts of the squeezed cores (data from Table 13). Dividing the total Cl or Br masses by the total mass of water yields the Cl and Br concentrations in bulk pore water. Under the assumption that the Cl and Br concentrations in water squeezed at the lowest pressure represent the in-situ concentrations in the free pore water, and conceptually dividing the pore water to a free-water reservoir that contains Cl and Br and a bound-water reservoir with zero Cl and Br content, the anion-accessible porosity fraction (AAPF) can be calculated by dividing the concentrations in bulk water by those in the squeezed water. The water, Cl and Br budgets, together with the obtained AAPF values, are listed in Table 15.

Table 14: Saturation Indices of Gypsum and Anhydrite in the Last APWs, in Squeezed Waters and in Aqueous Extracts of Squeezed Core

Type	ID	Sub-sample	SI (gypsum)	SI (anhydrite)	Data base
Last APW	BDR-B7 9.45	2A-16	-0.42	-0.61	Thermochimie
		3A-16	-0.40	-0.59	
		3B-16	-0.24	-0.42	
		4A-16	-0.43	-0.62	
		5A-16	-0.44	-0.63	
		6A-16	-0.43	-0.62	
	DGR-3-527.11	Slice 7A-15	0.03	-0.26	Pitzer
		Slice 8A-15	0.03	-0.26	
		Slice 9A-15	-0.03	-0.32	
		Slice 10A-15	0.00	-0.29	
		Slice 11A-15	0.04	-0.25	
		Slice 11B-15	0.05	-0.24	
		Slice 12A-15	0.03	-0.26	
	DGR-3-586.84	Slice 13A-15	-0.27	-0.55	
	DGR-4-637.03	Slice 19B-14	-0.41	-0.70	
		Slice 20A-14	-0.49	-0.78	
		Slice 22A-14	-0.32	-0.60	
		Slice 23A-14	-0.51	-0.80	
Squeezed water	BDR-B7 9.45	50 (lower)	-0.42	-0.61	Thermochimie
		50 (upper)	-0.45	-0.64	
		100	-0.35	-0.54	
		200	-0.35	-0.55	
		300	-0.29	-0.49	
		400	-0.26	-0.45	
		500	-0.22	-0.42	
	DGR-3 527.11	300	-0.11	-0.41	Pitzer
		400	-0.05	-0.34	
		500	-0.06	-0.35	
Aqueous extract of squeezed core	BDR-B7 9.45	a	-2.71	-2.90	Thermochimie
	DGR-3 527.11	a	0.08	-0.12	
		b	0.08	-0.12	
	DGR-3 586.84	a	-1.40	-1.60	
		b	-1.34	-1.54	
	DGR-4 637.03	a	-1.02	-1.22	
		b	-1.13	-1.33	

The following points can be made.

- The Cl-accessible porosity fraction of the Mont Terri sample is 0.68, which is slightly higher than the range 0.5–0.6 suggested by Pearson et al. (2003) for Opalinus Clay at Mont Terri. The reason for the relatively high value may be due to some degree of sample damage prior to the equilibration experiments or to the relatively high salinity used for the tests.

- For the Queenston Formation sample, Cl and Br can access the whole pore space, with no apparent exclusion. Note that this sample is the one with the lowest clay-mineral content

(Table 1). The Cl-accessible porosity fraction cannot exceed the value of 1, and the obtained value of 1.07 reflects methodological uncertainties.

- In the samples from the Georgian Bay and Blue Mountain Formations, a limited degree of anion exclusion is identified. The degree of anion exclusion depends on various factors, including the content of smectite and other minerals with a surface charge, the pore architecture and the pore-water salinity.

- For all samples, the accessibility for Br is slightly below that for Cl, consistent with the larger ionic radius of Br.

Table 15: Mass Balance of Cl and H_2O in Squeezed Cores, Calculation of the Anion-accessible Porosity Fraction (AAPF)

		Water budget			Cl budget			Br budget			Calculation of anion-accessible porosity fraction (AAPF)			
Sample	Water content after squeezing [wt.%]	Water mass squeezed [g]	Water mass remaining in squeezed sample (drying @ 105 °C) [g]	Total water mass in sample [g]	Cl squeezed [mg]	Cl remaining in squeezed sample (based on aq. extraction) [mg]	Total Cl in sample [mg]	Br squeezed [mg]	Br remaining in squeezed sample (based on aq. extraction) [mg]	Total Br in sample [mg]	Cl in bulk pore water [mg/kg]	Br in bulk pore water [mg/kg]	AAPF for Cl based on lowest squeezing pressure	AAPF for Br based on lowest squeezing pressure
BDR-B7-9.45	3.81	15.28	11.60	26.88	159.7	59.81	219.5	5.24	1.79	7.03	8167	261.5	0.68	0.62
DGR-3-527.11	2.72	1.08	11.83	12.91	99.54	1177	1277	3.42	37.86	41.28	98864	3196.8	1.07	1.00
DGR-3-586.84	2.81	4.62	10.31	14.93	418.3	860.7	1279	13.85	26.65	40.51	85645	2712.3	0.94	0.89
DGR-4-637.03	2.35	3.29	9.50	12.79	290.5	712.4	1003	10.07	23.41	33.48	78420	2618.1	0.88	0.86

7. COMPARISON OF THE CHEMICAL COMPOSITION OF THE SQUEEZED WATERS WITH THAT OF THE LAST APWS

In Table 16, the chemical compositions of waters squeezed at the lowest pressure step are compared with the last APW compositions, i.e. those taken at the time when the diffusion cells were disassembled. The comparison is also shown graphically in Figure 9 – Figure 12.

For the Mont Terri sample, water obtained at 50 MPa fits well with the APW composition for Na, Ca, Mg, Cl, Br and SO_4. Except for SO_4, the squeezed water has concentrations that are 0.9–6.2 $\%_{relative}$ below those in the last APW. Most likely, a limited degree of ion filtration affects the squeezed waters even in the first pressure step. The fact that Ca and Mg concentrations in the squeezed sample are not higher than in the APW is taken as an indication that pressure-induced carbonate mineral dissolution does not play a role at this pressure. The excellent correspondence of the SO_4 concentration indicates that no rock oxidation occurred since the disassembly of the diffusion cells (i.e., during handling, machining, transport and squeezing). Given the fact that K concentrations in the squeezed sample are close to the detection limit of

100 mg/kg (and below detection for all waters obtained at higher pressures), no conclusions pertinent to K can be made.

For the DGR samples, an excellent correspondence between squeezed waters and last APWs is seen for Na, Ca, Mg and Cl. Squeezed K is 6–9 $\%_{relative}$ below the APW value, probably due to the effects of ion filtration (due to the larger ionic radius, K is more strongly affected than Na). Br in waters squeezed from the Georgian Bay and Blue Mountain Formation samples is 5.2 $\%_{relative}$ below the values of the APW, again probably due to limited ion filtration. SO_4 concentrations are above detection only for the Queenston Formation sample, where the squeezed water has a content that is 26 $\%_{relative}$ below that of the APW. Given the fact that SO_4 concentrations are controlled by gypsum in this sample (Section 6.2.4), some SO_4 may have been removed by the precipitation of a sulphate mineral.

Overall, it is concluded that the squeezed waters are in excellent correspondence with the APWs, and that known artefacts have little or no effects on the results when the first squeezed water aliquot is considered. As shown in Section 8.2 and Table 12, waters obtained at higher pressure do show major deviations from the benchmarks for several solutes. Note that no conclusions can be drawn for pH, TIC and TOC. The APW samples were stored in 1.2 mL plastic containers (Cryovial® T310-1A from Simport Scientific Inc., Canada), and it turned out that these interact with the APWs over time and so render the measured values uncertain.

Table 16: Comparison of the Composition of the Last APW with That of the Water Squeezed at the Lowest Pressure

Sample	Side	Water type	Na [mg/kg]	K [mg/kg]	Ca [mg/kg]	Mg [mg/kg]	Cl [mg/kg]	Br [mg/kg]	SO_4 [mg/kg]
Opalinus Clay BDR-B7 9.45	A	Last APW (average of all slices used for squeezing)	7044		742.7	565.8	12686	439.5	1821
		Water squeezed at lowest pressure (50 MPa)	6740		696.7	560.8	11984	421.7	1835
		Relative difference to last APW [%]	-4.3		-6.2	-0.9	-5.5	-4.1	+0.8
Queenston Formation DGR-3 527.11	A/B	Last APW (average of all slices used for squeezing)	21699	2021	25751	2813	91386	3190	653.4
		Water squeezed at lowest pressure (300 MPa)	22154	1896	26057	2741	92166	3197	483.2
		Relative difference to last APW [%]	+2.1	-6.2	+1.2	-2.5	+0.9	+0.2	-26.0
Georgian Bay Formation DGR-3 586.84	A/B	Last APW (average of all slices used for squeezing)	22357	1979	25926	2882	94429	3216	
		Water squeezed at lowest pressure (200 MPa)	21636	1793	25832	2913	91478	3049	
		Relative difference to last APW [%]	-3.2	-9.4	-0.4	+1.1	-3.1	-5.2	
Blue Mountain Formation DGR-4 637.03	A/B	Last APW (average of all slices used for squeezing)	21904	1901	25664	2787	92919	3225	
		Water squeezed at lowest pressure (200 MPa)	21218	1783	24903	2711	89230	3057	
		Relative difference to last APW [%]	-3.1	-6.2	-3.0	-2.7	-4.0	-5.2	

8. MAIN EXPERIMENT: WATER ISOTOPES

8.1 RESULTS OF WATER ISOTOPIC MEASUREMENTS

8.1.1 Water Isotopes in APWs

As for the chemical compositions, the water isotopic compositions of the APW were monitored over the entire duration of the experiment. Given the small water volume of 0.5 mL extracted for each monitoring step, 1.2 mL plastic cryovials were used as sample containers (details in Section 7). The isotope analyses of these waters yielded erratic and unplausible results that are not reported here. While the CRDS analytics worked well and yielded consistent results that were checked by recurrent measurement of the pure APW, the storage of the waters over weeks to months in the plastic cryovials resulted in major artefacts. In another project that was running in our institute at the same time, a systematic dependence between the size of the plastic vials and the isotopic composition was observed, with major deviations from the

expected values for the smallest vials, i.e., those with the largest surface to volume ratio (Mazurek et al. 2018).

While the data for the time series are not meaningful, the initial APWs as well the last ones that were collected at the time when the diffusion cells were disassembled were stored in glass containers and so were not affected by this type of artefact. These data are meaningful and are reported here. Also note that all squeezed waters as well those obtained by the AIDE method (see below) were always stored in glass vessels and never in contact with plastic, so they are considered to be useful.

The water isotopic compositions of the last APWs for all samples (5–6 slices each) are listed in Table 17. For each sample, the data for all slices vary only marginally (except 1 slice from sample DGR-3 527.11), indicating that no leakage occurred from the cells.

8.1.2 Water Isotopes in Squeezed Waters

The isotopic composition of squeezed waters is listed in Table 17. The variation of the data with squeezing pressure is marginal and not systematic. It appears that even data obtained at high squeezing pressures are useful, in contrast to the chemical composition.

8.1.3 Water Isotopes Based on the AIDE Method

In accordance with de Haller et al. (2016), two isotope exchange experiments per sample were performed, one with a test water with an isotopic composition close to local tap water (LAB), and a second with glacial water (SSI). As shown in Table 18, the total mass (rock + water) changed only marginally over the experiment, confirming the tightness of the system. A limited mass transfer from the test water to the rock sample occurred (Table 18), but experience shows that this does not affect the results as long as the transfer stays below 10 %. For the SSI experiment with sample DGR-4 637.03, a more substantial transfer occurred, and drops of water were identified on the rock sample at the end of the experiment (and dripped into the container during dismantling).

Based on the measured isotopic composition of the test waters, the composition of the original pore water was calculated using the formalism of Rübel et al. (2002) and is listed in Table 17. Furthermore, a water content can be obtained on the basis of a mass-balance calculation and is listed in Table 18. It is in reasonable agreement with the gravimetric water content listed in Table 1.

Table 17: Water Isotopic Composition of the Last APWs (all slices) and of Squeezed Waters, Together with the Results Based on the AIDE Technique

Sample	Water type	Slice	Side	Lab ID	Squeezing pressure [MPa]	δ18O [‰V-SMOW]	Error [‰V-SMOW]	δ2H [‰V-SMOW]	Error [‰V-SMOW]
BDR-B7-9.45	APW	2	A	2A-16		-10.20	0.07	-73.0	0.2
		3	A	3A-16		-10.28	0.06	-73.6	0.3
		3	B	3B-16		-10.27	0.05	-73.8	0.3
		4	A	4A-16		-10.27	0.01	-73.3	0.4
		5	A	5A-16		-10.25	0.05	-73.2	0.2
		6	A	6A-16		-10.24	0.04	-73.1	0.3
	Squeezed	3 to 6			50	-9.91	0.02	-71.4	0.3
					50	-9.81	0.03	-71.2	0.4
					100	-9.95	0.09	-71.6	0.3
					200	-10.09	0.05	-72.2	0.4
					300	-10.15	0.05	-72.5	0.4
					400	-10.23	0.04	-72.9	0.3
					500	-10.18	0.03	-72.7	0.1
	Diff. exchange	2				-9.73	0.19	-72.4	1.9
DGR-3-527.11	APW	7	A	7A-15		-9.77	0.04	-74.5	0.3
		8	A	8A-15		-9.78	0.02	-74.8	0.1
		9	A	9A-15		-9.77	0.03	-74.8	0.3
		10	A	10A-15		-9.82	0.14	-75.0	0.4
		11	A	11A-15		-9.79	0.10	-74.9	0.1
		11	B	11B-15		-9.71	0.12	-74.7	0.3
		12	A	12A-15		-10.18	0.10	-75.5	0.6
	Squeezed	7 to 9, 11 to 12			300	-8.36	0.06	-70.4	0.1
					400	-9.00	0.03	-71.5	0.3
					500	-8.61	0.09	-71.1	0.3
	Diff. exchange	10				-9.13	0.26	-71.7	2.4
DGR-3-586.84	APW	13	A	13A-15		-9.37	0.07	-73.6	0.4
		14	A	14A-15		-9.43	0.06	-73.4	0.4
		15	A	15A-15		-9.53	0.12	-73.8	0.3
		16	A	16A-15		-9.66	0.12	-74.0	0.3
		16	B	16B-15		-9.56	0.06	-73.6	0.1
		17	A	17A-15		-9.69	0.15	-74.2	0.2
	Squeezed	13 to 16			200	-9.06	0.02	-72.2	0.5
					300	-9.02	0.03	-71.3	0.1
					400	-8.99	0.12	-71.3	0.3
					500	-8.91	0.06	-70.7	0.2
	Diff. exchange	17				-9.01	0.28	-71.9	2.6
DGR-4-637.03	APW	18	A	18A-14		-9.50	0.11	-73.4	0.3
		19	A	19A-14		-9.55	0.11	-73.7	0.4
		19	B	19B-14		-9.48	0.09	-73.5	0.2
		20	A	20A-14		-9.78	0.15	-74.4	0.3
		21	A	21A-14		-9.53	0.04	-74.1	0.7
		22	A	22A-14		-9.77	0.04	-74.6	0.2
		23	A	23A-14		-9.74	0.04	-74.8	0.2
	Squeezed	19 to 23			200	-8.87	0.14	-71.2	0.3
					300	-9.10	0.05	-71.8	0.4
					400	-9.15	0.08	-72.0	0.1
					500	-9.22	0.15	-72.0	0.1
	Diff. exchange	18				-8.98	0.31	-72.0	2.8

Table 18: Experimental Details and Calculated Water Content Based on the AIDE Technique

Sample	Slice	Initial LAB water mass	Initial SSI water mass	Initial LAB rock mass	Initial SSI rock mass	Total mass change (rock + water) over LAB experiment	Total mass change (rock + water) over SSI experiment	Mass change of test water LAB over the experiment		Mass change of test water SSI over the experiment		Wet water content (calculated)	Error
		g		g		g		g	%	g	%	wt.%	
BDR-B7-9.45	2	7.214	7.083	138.733	136.282	0.005	0.011	-0.170	-2.4	-0.153	-2.2	9.08	0.22
DGR-3-527.11	10	4.188	3.306	88.350	103.846	-0.029	-0.027	-0.308	-7.4	-0.281	-8.5	4.12	0.12
DGR-3-586.84	17	4.178	4.182	90.112	110.956	-0.028	-0.012	-0.323	-7.7	-0.352	-8.4	3.29	0.09
DGR-4-637.03	18	4.189	4.180	92.205	91.978	-0.028	-0.155	-0.281	-6.7	-0.569	-13.6	3.67	0.09

9. COMPARISON OF THE WATER ISOTOPIC COMPOSITION BASED ON SQUEEZING AND AIDE WITH THAT OF THE LAST APWS

The water isotopic data listed in Table 17 are shown graphically in Figure 14. Note that analytical errors are shown for the APW and squeezing data, while the propagated total error is indicated for the AIDE results. The following observations can be made.

- Water isotopic compositions obtained by squeezing and AIDE are identical within error. The only exception is the Queenston Formation sample DGR-3 527.11, in which $\delta^{18}O$ values of squeezed waters deviate towards higher values. This is probably an artefact due to evaporation, given the fact that water masses squeezed from this sample were quite low (only 0.34–0.38 mL per pressure step, see Table 11).

- For the DGR samples, δ values obtained by squeezing and AIDE are both consistently higher when compared with the last APW. For the clay-rich samples from the Georgian Bay and Blue Mountain Fm., the deviation is 0.5–0.7 ‰ for $\delta^{18}O$ and 1.6–2.8 ‰ for $\delta^{2}H$. For the clay-poor sample from the Queenston Formation, it is more substantial (0.7–1.5 ‰ for $\delta^{18}O$ and 3.2–4.5 ‰ for $\delta^{2}H$). The slope of the deviation is smaller than that of the meteoric water line (Figure 14). It is suspected that the shift is due to effects of evaporation since the time when the diffusion cells were disassembled, and that evaporation affects both the squeezing and AIDE data to comparable degrees. Nevertheless, given the difficulties related to the measurement of the water isotopic composition of highly saline pore waters in consolidated shales, the deviation from the benchmark appears acceptable.

- For the Mont Terri sample, the same shift away from the APW is seen as for the DGR samples, but it is less strongly expressed. Given the higher water content, potential effects of evaporation become less relevant for both the squeezing and the AIDE techniques. The deviation from the APW composition is 0.3–0.5 ‰ for $\delta^{18}O$ and 0.9–2.1 ‰ for $\delta^{2}H$.

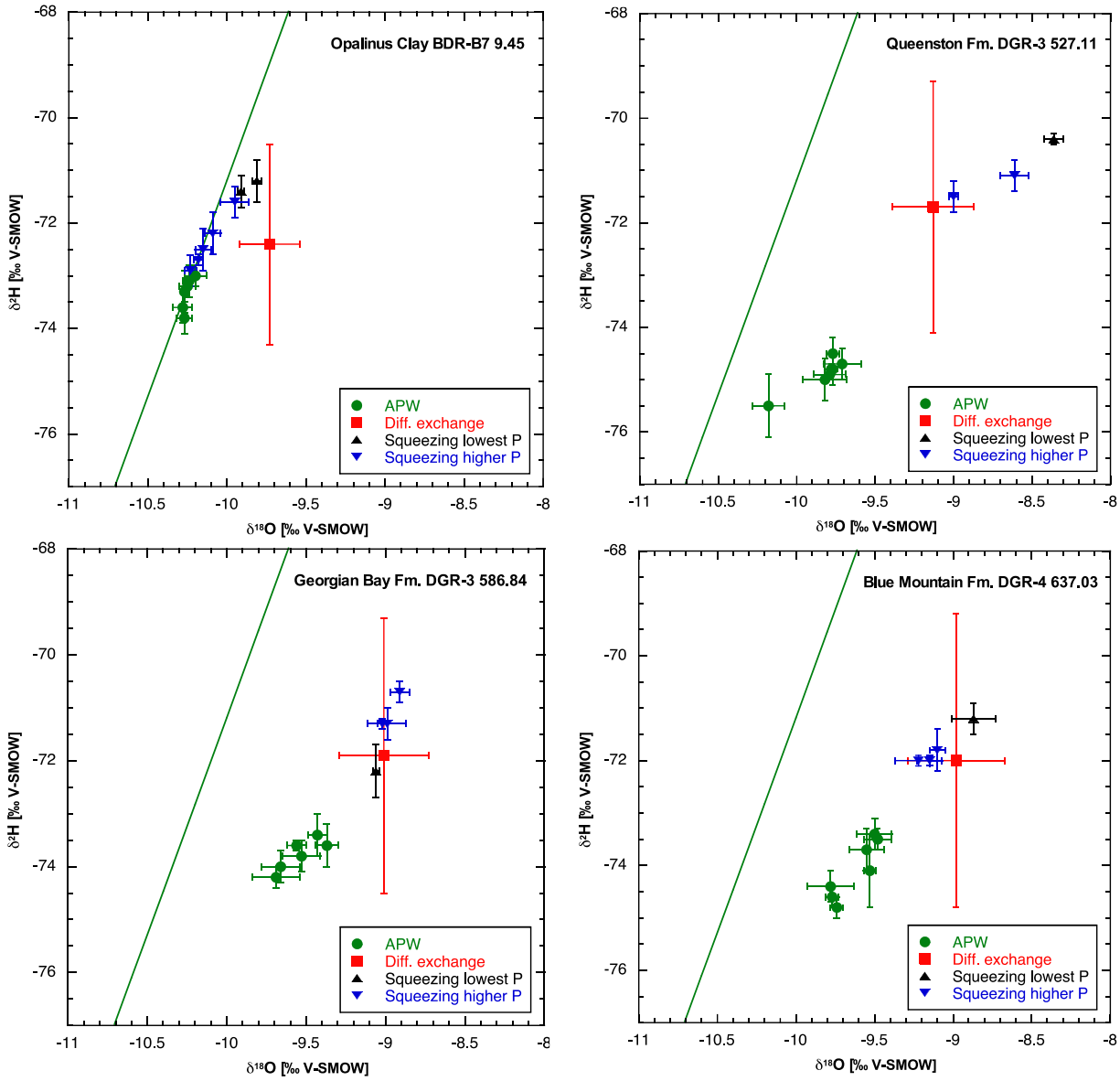

Notes: Green line indicates the Global Meteoric Water Line.

Figure 14: Comparison of Water Isotopic Compositions of the Last APWs with Data from Squeezing and AIDE

10. CONCLUSIONS

In the frame of a method benchmarking exercise, equilibrated rock samples were subjected to squeezing (major ion chemistry analyses by ion chromatography and stable water isotopic analyses by CRD spectroscopy) and adapted isotope diffusive exchange (AIDE) experiments (stable water isotopic analyses by CRD spectroscopy). Diffusion cells were designed to equilibrate the pore water within rock slices with an external reservoir. The cells provided volumetric confinement for swelling materials. Given the fact that steel was avoided and all parts in contact with water were made of plastic or titanium, the cells were also suited for highly

saline and therefore corrosive systems. The time needed for sufficient equilibration depends on how close the chemical and isotopic compositions of the external reservoir are to the original pore water. While the experiments could not be performed under controlled atmosphere, only a small number of cells showed indications of limited oxidation (e.g. increasing SO_4 and Ca contents). Most cells were unaffected by oxidation, i.e., tight over the time of the experiment. In future experiments when the acquisition of time-series data may not be necessary, the cells might be placed in a glovebox for the entire equilibration time.

Major Ion Chemistry

For the Opalinus Clay sample, the first water was obtained by squeezing at a pressure of 50 MPa. For Na, Ca, Mg, Cl, Br and SO_4, the composition of the squeezed water corresponds within ±6 % to the composition of the last APW, i.e., the water that actually resided in the sample before squeezing. For methodological reasons, no conclusions can be drawn about K and pH. For the DGR samples, Na, Ca, Mg, Cl and Br in the first squeezed water (obtained at 200–300 MPa) are within ±5 % of the last APWs. Squeezed K is 6–9 % below the benchmark value, possibly due to the effects of ion filtration. SO_4 is below detection except in the Queenston Formation sample, where the squeezed water has a SO_4 content 26 % below that of the last APW. While this discrepancy is not fully understood, it may be related to the precipitation of small amounts of gypsum, given the fact that all waters of this sample are gypsum-saturated and the rock contains traces of anhydrite.

Stable Water Isotopes

Water isotopic data obtained by squeezing and AIDE experiments were compared to the composition of the last APWs. For the Opalinus Clay sample (clay content 66 %), $\delta^{18}O$ and $\delta^{2}H$ are 0.3–0.5 ‰ and 0.9–2.1 ‰ higher than the last APW, respectively. The difference is larger (0.5–0.7 ‰ and 1.6–2.8 ‰ for $\delta^{18}O$ and $\delta^{2}H$, respectively) for the Georgian Bay and Blue Mountain Fm. samples (clay content 63–65 %) and reach as high as 0.7–1.5 ‰ and 3.2–4.5 ‰, respectively, for the Queenston Formation sample (clay content 47 %). As the squeezing and AIDE data deviate to the right of the Global Meteoric Water Line, it is suspected that evaporation affects the results to a limited degree. This effect is small for the Opalinus Clay sample, with its high water content, and is most strongly expressed in the low-porosity and relatively low clay-content Queenston Formation sample.

REFERENCES

de Haller, A., M. Hobbs and J.E. Spangenberg. 2016. Adapting the diffusive exchange method for stable isotope analysis of pore water to brine-saturated rocks. Chem. Geol. 444: 37–48.

Fernández, A.M., D.M. Sánchez-Ledesma, C. Tournassat, A. Melón, E. Gaucher, J. Astudillo and A. Vinsot. 2014. Applying the squeezing technique to highly consolidated clayrocks for pore water characterisation: lessons learned from experiments at the Mont Terri rock laboratory. Appl. Geochem. 49: 2–21.

Giffaut, E., M. Grivé, P. Blanc, P. Vieillard, E. Colàs, H. Gailhanou, S. Gaboreau, N. Marty, B. Madé and L. Duro. 2014. Andra thermodynamic database for performance assessment: ThermoChimie. Appl. Geochem. 49: 225–236.

Giger, S. and P. Marschall. 2014. Geomechanical properties, rock models and in-situ stress conditions for Opalinus Clay in Northern Switzerland. Nagra Arbeitsbericht NAB 14-01, Nagra, Wettingen, Switzerland.

Heagle, D. and L. Pinder. 2009. Opportunistic Groundwater Sampling in DGR-3 and DGR-4. Intera Technical Report TR-08-18.

Hobbs, M., A. de Haller, M. Koroleva, M. Mazurek, J. Spangenberg, U. Mäder and D. Meier. 2011. Borehole DGR-3 and DGR-4 Porewater Investigations. Geofirma Technical Report TR-08-40. Toronto, Canada.

Lichtner, P.C. 2004. Flotran User's Manual: Two phase, non-isothermal coupled thermal-hydrologic-chemical (THC) reactive flow and transport code. LANL Rep. LA-UR-01-2349, Los Alamos National Laboratory, Los Alamos, NM, USA.

Mazurek, M., T. Oyama, F. Eichinger and A. de Haller. 2013. Squeezing of porewater from core samples of DGR boreholes: Feasibility study. NWMO TR-2013-19. Toronto, Canada

Mazurek, M., T. Oyama, P. Wersin and P. Alt-Epping. 2015. Pore-water squeezing from indurated shales. Chem. Geol. 400: 106–121.

Mazurek, M., T. Oyama, U. Mäder and H.N. Waber. 2017. Squeezing of pore water from Opalinus Clay: Effects of sample preparation and comparison with alternative sampling methods. Nagra Arbeitsbericht NAB 16-69. Wettingen, Switzerland.

Mazurek, M., P. Wersin and J. Hadi. 2018. Opalinus Clay in the shallow decompaction zone: Geochemical investigations on drill core samples from borehole Lausen KB. Nagra Arbeitsbericht NAB 16-58. Wettingen, Switzerland.

Nagra. 2014. SGT Etappe 2: Vorschlag weiter zu untersuchender geologischer Standortgebiete mit zugehörigen Standortarealen für die Oberflächenanlage – Geologische Grundlagen. Dossier VI: Barriereneigenschaften der Wirt- und Rahmengesteine. Nagra Technical Report NTB 14-02.

Parkhurst, D. L. and C.A.J. Appelo. 2013. Description of input and examples for PHREEQC version 3 — a computer program for speciation, batch-reaction, one-dimensional transport,

and inverse geochemical calculations. U.S. Geological Survey Techniques and Methods, Book 6, Chap. A43 (497 pp. Available at http://pubs.usgs.gov/tm/06/a43).

Pearson, F.J., D. Arcos, A. Bath, J.Y. Boisson, A.M. Fernández, H.E. Gaebler, E.C. Gaucher, A. Gautschi, L. Griffault, P. Hernan and H.N. Waber. 2003. Mont Terri Project - Geochemistry of Water in the Opalinus Clay Formation at the Mont Terri Rock Laboratory. Reports of the Federal Office of Water and Geology (FOWG), Geology Series No. 5.

Rogge, T. 1997. Eine molekular-diffusive Methode zur Bestimmung des Porenwassergehaltesund der Zusammensetzung von stabilen Isotopen im Porenwasser von Gestein. Diploma thesis, University of Heidelberg, Germany (unpublished).

Rübel, A.P., C. Sonntag, J. Lippmann, F.J. Pearson and A. Gautschi. 2002. Solute transport informations of very low permeability: profiles of stable isotope and dissolved noble gas contents of pore water in the Opalinus Clay, Mont Terri, Switzerland. Geochim. Cosmochim. Acta 66: 1311–1321.

Vinsot, A., C.A.J. Appelo, C. Cailteau, S. Wechner, J. Pironon, P. De Donato, P. De Cannière, S. Mettler, P. Wersin and H.E. Gäbler. 2008. CO_2 data on gas and pore water sampled in situ in the Opalinus Clay at the Mont Terri rock laboratory. Phys. Chem. Earth 33: S54–S60.

Waber, H.N., U.K. Mäder, M. Koroleva and A. de Haller. 2007. Testing Methods for the Characterisation of Saline Pore Water in an Ordovician Limestone (Cobourg Formation, St. Mary's Quarry, Ontario). Rock-Water Interaction (RWI), Institute of Geological Sciences, University of Bern, Switzerland, TR-07-01, 112 p.

Wersin, P., M. Mazurek, H.N. Waber, U.K. Mäder, T. Gimmi, D. Rufer and A. de Haller. 2013. Rock and porewater characterisation on drillcores from the Schlattingen borehole. Nagra Arbeitsbericht NAB 12-54. Wettingen, Switzerland.

Xiang, Y., T. Al and M. Mazurek. 2016. Effect of confining pressure on diffusion coefficients in clay-rich, low-permeability sedimentary rocks. J. Contam. Hydrol. 195: 1–10.